THE ROLE AND EFFECT OF DAMPING ON THE RESPONSE OF A FLEXIBLE SHAFT IN THE REGION OF A CRITICAL SPEED

****

A THESIS

PRESENTED TO

THE FACULTY OF THE DEPARTMENT OF MECHANICAL ENGINEERING

UNIVERSITY OF HOUSTON

****

IN PARTIAL FULFILMENT

OF THE REQUIREMENTS FOR THE DEGREE

MASTER OF SCIENCE IN MECHANICAL ENGINEERING

****

BY

CHIA-CHIH CHANG

JANUARY 1969

ACKNOWLEDGMENTS

The author wishes to express his deepest gratitude to Dr. D. Muster, his advisor, for suggesting the topic of this experimental study as well as for his advice, assistance and very careful inspirarion which aided in the completion of this work.

Beyond this the author is indebted to others of the faculty and his colleagues for their assistance; for this he is most grateful.

THE ROLE AND EFFECT OF DAMPING ON THE RESPONSE OF A FLEXIBLE SHAFT IN THE REGION OF A CRITICAL SPEED

****

AN ABSTRACT OF A THESIS

PRESENTED TO

THE FACULTY OF THE DEPARTMENT OF MECHANICAL ENGINEERING

UNIVERSITY OF HOUSTON

****

IN PARTIAL FULFILMENT

OF THE REQUIREMENTS FOR THE DEGREE

MASTER OF SCIENCE IN MECHANICAL ENGINEERING

****

BY

CHIA-CHIH CHANG

JANUARY 1969

ABSTRACT

An experimental study concerned with the role and effect of damping for a rotating flexible shaft in the region of a critical speed is conducted. The existing theory [1]* is reviewed for a rotating system with an unbalanced disk in the center of a flexible shaft. The effect of damping on the system is discussed. The experimental results reveal that the external damping plays a role which is taken properly into account by the existing theory. In contract, internal damping does not affect the rotating system in the region of the critical speed.

* Numbers in brackets refer to corresponding references in the bibliography.

TABLE OF CONTENTS

LIST OF TABLES

LIST OF FIGURES

LIST OF SYMBOLS

a	internal damping constant
c	decay constant of a viscous damping system
i	imaginary number
k	lateral stiffness of the shaft
l	length of shaft between bearings
m	mass of disk
t	time
x, y	coordinate of geometrical center
z	complex vector of the displacement in stationary system of coordinate
A_R	amplification factor
A_1 A_2	constant of integration
C	viscous damping coefficient
C_c	critical damping constant
C_{eq}	equivalent viscous damping constant
E	Young's modulus
F_d	internal damping force
G	mass center of the disk
I	moment of inertia
O	intersection point of the bearings center with the disk
R	deflected distance
S	geometrical center of the disk
U	work done per cycle at resonance

X, Y	stationary system of coordinate
ζ	complex vector of the displacement in rotating system of coordinate
η, ξ	rotating system of coordinate
λ_1, λ_2	roots of the characteristic equation
ρ	radial distance from S
ψ	damping ratio
ω	angular velocity of the shaft
ω_A	circular frequency of peak response near resonance
ω_n	natural frequency of lateral vibration
ω_o	natural frequency of the damped vibrations of the system

CHAPTER I

THEORY

<u>General</u> All material used to construct machinery possess mass and elasticity which always makes vibration possible. A rotating shaft with mass unbalance, no axial symmetry or subjected to such external factors as gyroscopic forces, friction in the bearings, etc. tends to whirl at certain speeds.

Since the bearing supports are relatively rigid, the forces exerted on the bearings are due to centrifugal force caused by the unbalance. The shaft for which the dynamic

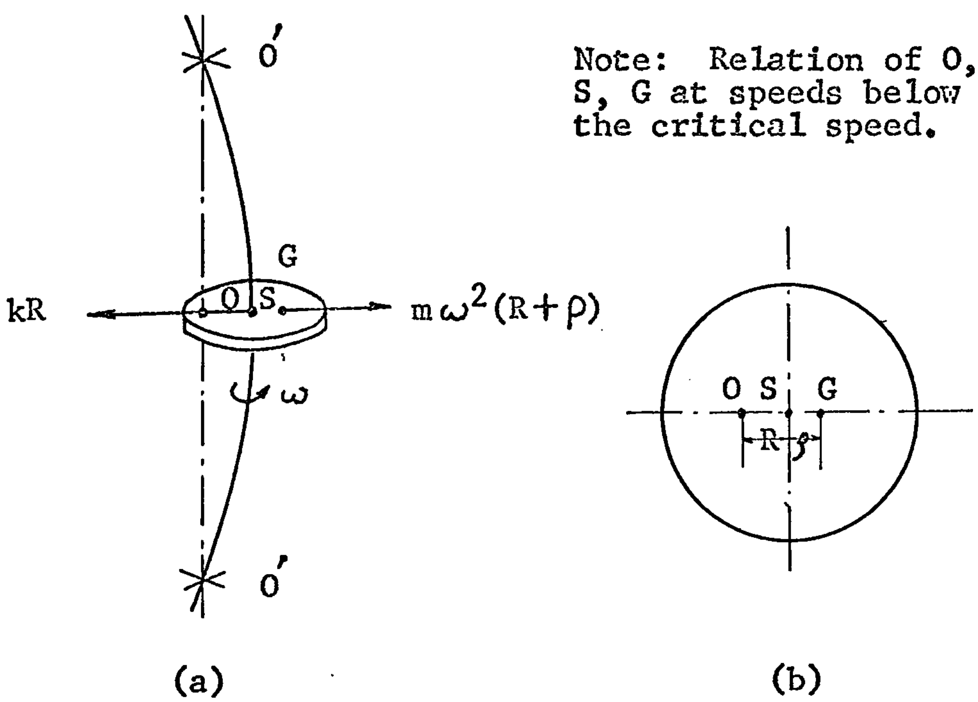

Fig. 1 Deflection of a shaft due to mass unbalance

action and interaction of shaft elasticity, bearing elasticity, and damping must be considered is called flexible.

When the shaft-disk system of Figure 1 is rotated, a speed-depended centrifugal force acts on the mass center, causing it to move outward under the restraining influence of a restoring force offered by the stiffness of the shaft (Equation (1)). In an undamped system a speed characterized by Equation (1), there is a speed for which equilibrium is not possible. This speed is called the critical speed and is denoted by ω_n. It corresponds to a resonant frequency of the system. In the case of the system in Figure 1, it corresponds to the lowest bending mode of the shaft [2].

In a rotating shaft and vibrating systems, friction is always present and offers resistance to motion. The resistance in such systems usually restricts the vibratory motion in the region of the critical speeds and the natural frequencies. The friction in a rotating shaft system which includes the bearings and supports has a special character. The friction which can be attributed to interaction between the rotating and the stationary parts is called external friction, and the friction within the rotating parts alone is called internal friction.

Internal friction (damping) for a rotating system usually includes two fundamental components: hysteretic damping and structural damping. The latter is caused by micro-shifts between individual parts of the rotating system. The most frequent cause of such structural damping is dry friction which occurs at the juncture of the hub of the disk and the shaft. The factors which affect hysteretic damping include the amplitude and frequency of the vibratory motion and temperature. Of these, it has been shown that the vibration amplitude is usually the most important.

In order to isolate and identify these parameters in the study reported here air bearings (which are characterized by low-friction) were used. These included externally pressurized journal and thrust bearings. As a consequence, the role and effect of internal damping in the shaft may be determined experimentally.

A. Whirling without damping [3]

First, whirling without damping is considered. Consider idealized system, which consists of a single disk with a mass m located firmly and symmetrically on a vertical shaft supported by two bearings (Figure 1). Because of mass unbalance, the mass center G of the disk is at a radial distance ρ from the geometrical center S of the disk. During rotation, the center line of the bearings intersects the plane of the disk at O,(this is defined as the spin axis). With respect to the spin axis, the shaft center is deflected a distance $\overline{OS}$, say R.

If the effect of friction is neglected, the disk is under the action of two forces: the restoring force of the shaft,

(=kR, where k is the lateral stiffness of the shaft at the disk), and the centrifugal force of the mass, $m\omega^2(R+\rho)$. In an undamped system, when these two forces are in equilibrium, they are collinear, equal in magnitude, and opposite in direction as shown in Figure 1 (a). This may be stated as

$$kR = m\omega^2(R+\rho) \tag{1}$$

From which we obtain

$$R = \frac{m\omega^2\rho}{k - m\omega^2} \tag{2}$$

Equilibrium is not possible at speeds for which $k - m\omega^2 = 0$; thus, at values of $\omega^2 = k/m$ $(\equiv\omega_n^2)$ the deflection of the shaft becomes (in theory) infinitely large. We call this the critical speed of the shaft. For a one-degree-of-freedom system of mass m and stiffness k, the undamped natural frequency is also defined as $\omega_n = \sqrt{k/m}$ (4). For this reason critical speed is defined as "... a speed of a rotating system that corresponds to a resonance frequency of the system." (5)

On the basis of the above we denote the critical speed of the rotating system by ω_n. It also shows that R is positive when ω is below ω_n and that R is negative when ω is greater than ω_n. Thus, for $\omega < \omega_n$ the system rotates with the mass center outside OS, (i.e. G outside S as shown in Fig. 2 (a)) and that for $\omega > \omega_n$ the mass center is between O and S and on OS (i.e. S is outside G as shown in Fig. 2 (b)).

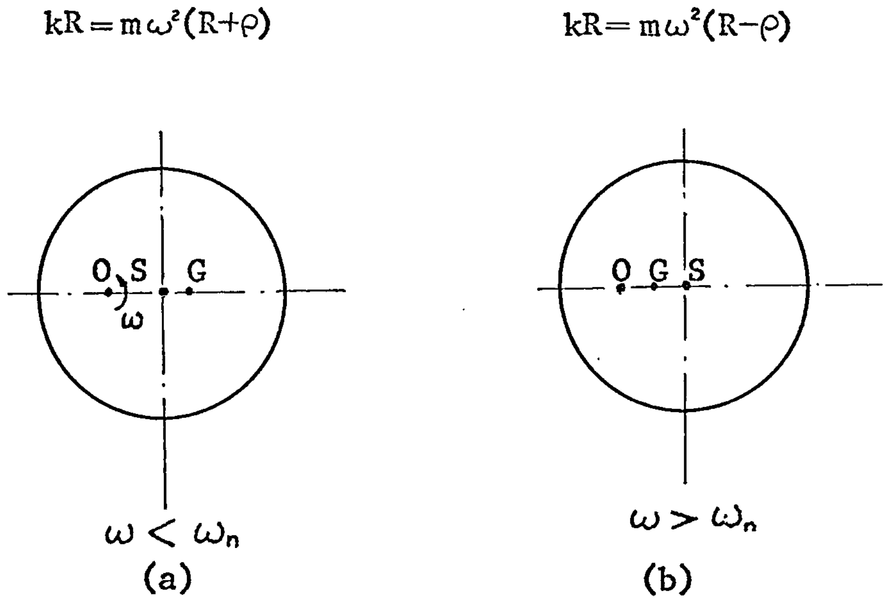

Fig. 2 The relation between the mass center geometric center, and spin axis of a disk during rotation

When ω is very much greater than ω_n, the deflection R approaches $-\rho$ and the points O and G are in essential coincidence; thus, disk tends to rotate about its mass center G. This process is called mass centering.

B. Whirling with damping

Since there is no first-order alternating stress in the rotating system at or near the critical speed, then material damping cannot aid materially in limiting excessive deflection of the system. The converse is true for lateral vibration of the same system at a resonant frequency. This places special importance on the damping furnished by the bearings and their supports. The factors that limit amplitude at critical speeds are mainly nonlinear effects in elastic properties of the system and damping in the bearings — the latter mainly due to motions and interaction effects at frequencies other than at running speed.

Although it is assumed here that the rotating shaft-bearing system does not vibrate, it is caused to vibrate at speeds other than the running speed (some times excessively) by dynamic actions characteristic of fluid-film lubrication. There are two distinguishable vibration phenomena, one called half-frequency whirl, another called resonantwhip (6). Whirl may occur with relatively stiff rotating systems at any speed; it has a vibration frequency at or near half the running speed. Whip may occur with flexible rotating systems at speeds equal to or above twice the first critical speed of the rotating shaft-bearing system; it has a vibration frequency equal or very nearly equal to the first critical speed. The literature which covers this more general problem, the dynamic behavior, of rotor-bearing systems, extends to the effects of critical speeds, bearing instability, and the influences of bearing parameters on rotor behavior, in addition to balancing (6).

In the region of the critical speed of a damped rotating system, there is a new relation between points O, S, and G (as is shown in Figure 3).

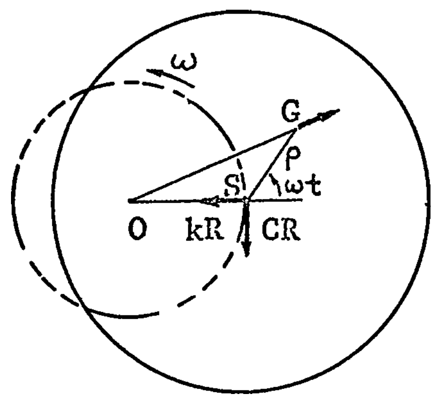

Restoring force

Centrifugal force

Friction force

Fig. 3 Whirling of shaft due to mass unbalance when friction force is considered

After Tondl (1), the problen may be considered as the motion in the XY-plane of a disk on which is impressed a constant angular speed ω. He shows that the equation of motion of the system with mass m in X-direction (Fig. 3) is

$$m\frac{d^2}{dt}(x+\rho\cos\omega t)+C\frac{dx}{dt}+kx=0 \tag{3}$$

and the equation of motion of m in Y-direction is

$$m\frac{d^2}{dt}(y+\rho\sin\omega t)+C\frac{dy}{dt}+ky=0 \tag{4}$$

where C is the viscous damping coefficient. Since the disk revolves at a constant angular velocity ω, this circumstance must be taken into account with expressing the force of internal damping (1); consequently, it will be advantageous to introduce a rotating system of coordinates ξ and η which revolves at the angular velocity ω as shown in Fig. 4. In place of the deflections x, y, and ξ , η , it is possible to

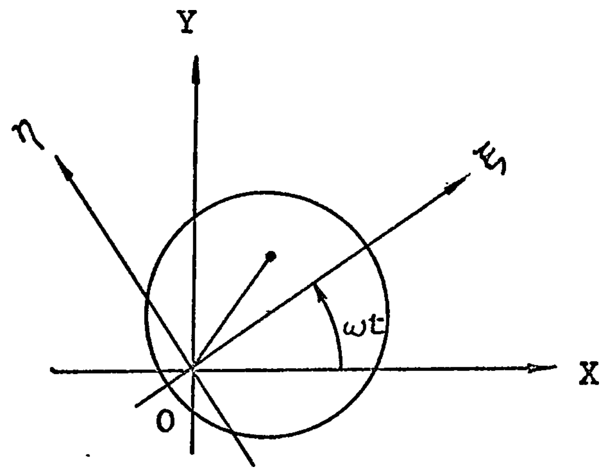

Fig. 4 Coordinate systems relation

introduce the complex vectors z and ζ. Where,

$$z = x + iy \qquad \text{and} \qquad \zeta = \xi + i\eta \tag{5}$$

The equation of motion in the rotating coordinate system may be written as

$$m(\ddot{\zeta} + 2i\omega\dot{\zeta} - \omega^2\zeta) + C(\dot{\zeta} + i\omega\zeta) + k\zeta = m\rho\omega^2 \tag{6}$$

If it is assumed that the internal damping introduced into the system is proportional to the square of the amplitude with respect to the rotating coordinate system (7) and using the concept of equivalent viscous dampin (3), it is possible to write

$$F_d = -C_{eq}\dot{\zeta} \tag{7}$$

where

$$C_{eq} = \frac{4}{3\pi} a \omega R \quad * \tag{8}$$

Therefore, the general equation of motion with internal damping in the rotating coordinate system may be written as

$$\ddot{\zeta} + 2i\omega\dot{\zeta} - \omega^2\zeta + c(\dot{\zeta} + i\omega\zeta) + c_{eq}\dot{\zeta} + \omega_n^2\zeta = \rho\omega^2 \tag{9}$$

where

$$c = C/m, \quad c_{eq} = C_{eq}/m, \quad \omega_n^2 = k/m$$

In terms of the stationary coordinates, Equation (9) becomes

$$\ddot{z} + c\dot{z} + c_{eq}(\dot{z} - i\omega z) + \omega_n^2 z = \rho\omega^2 e^{i\omega t} \tag{10}$$

A particular solution of which is

$$z = \frac{\rho\omega^2}{\omega_n^2 - \omega^2 + ic\omega} e^{i\omega t} \tag{11}$$

or in the rotating coordinates

$$\zeta = \frac{\rho\omega^2}{\omega_n^2 - \omega^2 + ic\omega} (= R) \tag{12}$$

If the phase relation is neglected, R represents the rotating circle of the system due to mass unbalance. The magnitude of ζ in Equation (12) can be written

$$|\zeta| = \frac{\rho\left(\frac{\omega}{\omega_n}\right)^2}{\sqrt{\left[1 - \left(\frac{\omega}{\omega_n}\right)^2\right]^2 - \left(\frac{\omega}{\omega_n}\right)^2\left(\frac{c}{\omega_n}\right)^2}} \tag{13}$$

* Appendix I

This shows that external friction leads to damping of the natural vibrations and to a restriction of the amplitudes of the motion in the region of critical speeds. It appears that the motion caused by mass unbalance is not affected by internal damping; however, the general solution of Equation (10) shows that c_{eq} does influence the system during rotation.

The homogeneous solution of Equation (10) may be written as

$$z = A_1 e^{i\lambda_1 t} + A_2 e^{i\lambda_2 t} \tag{14}$$

Where A_1 and A_2 are constants of integration and λ_1 and λ_2 are roots of the characteristic equation

$$\lambda^2 - i\lambda(c + c_{eq}) - \omega_n^2 + i c_{eq}\omega = 0 \tag{15}$$

The solution of Equation (15) will be

$$\lambda_{1,2} = \frac{1}{2} i (c + c_{eq}) \pm \sqrt{\omega_n^2 - \frac{1}{4}(c + c_{eq})^2 - i c_{eq}\omega} \tag{16}$$

Let ω_0 be the natural frequency of the damped vibrations of the system where

$$\omega_0^2 = \omega_n^2 - \frac{1}{4}(c + c_{eq})^2$$

For $c_{eq}\omega \ll \omega_0^2$

$$\sqrt{\omega_0^2 - i c_{eq}\omega} \doteq \omega_0 - \frac{1}{2} i c_{eq} \frac{\omega}{\omega_0}$$

and λ_1 and λ_2 may be written approximately as

$$\lambda_1 \doteq \omega_0 + \frac{1}{2} i\left(c + c_{eq} - \frac{c_{eq}\omega}{\omega_0}\right) \tag{16-a}$$

$$\lambda_2 \doteq -\omega_0 + \frac{1}{2} i\left(c + c_{eq} + \frac{c_{eq}\omega}{\omega_0}\right) \tag{16-b}$$

and the solution of the homogeneous equation (10) is

$$z = A_1 e^{\left(i\omega_0 - \frac{1}{2}\left\{c + c_{eq} - \frac{c_{eq}\omega}{\omega_0}\right\}\right)t} + A_2 e^{\left\{-i\omega_0 - \frac{1}{2}\left(c + c_{eq} + \frac{c_{eq}\omega}{\omega_0}\right)\right\}t} \tag{17}$$

The effect of internal damping may be examined qualitatively from Equations (16-a) and (16-b). If

$$\omega < \omega_0\left(1 + \frac{c}{c_{eq}}\right) \tag{18}$$

then both terms on the right hand side of Equation (17) converge with increasing time, i.e.

$$\lim_{t\to\infty} z = 0$$

This implies that the internal damping plays a role as a resistance effect. However, if the inequality (18) does not hold, and

$$\omega > \omega_0\left(1 + \frac{c}{c_{eq}}\right) \tag{19}$$

then, it follows that

$$\lim_{t\to\infty} z = 0$$

It follows that if the inequality (18) is not satisfied the internal damping does not play a role as a resistance effect. and, in fact, may induce the system to vibrate infinitely.

Obviously, from the analysis, it shows that the vibration of a rotating shaft system with mass unbalance is affected by the existence of damping. External damping tends to restrict the deflection of the shaft in the region of a critical speed; internal damping does the same thing only when equation (18) satisfied.

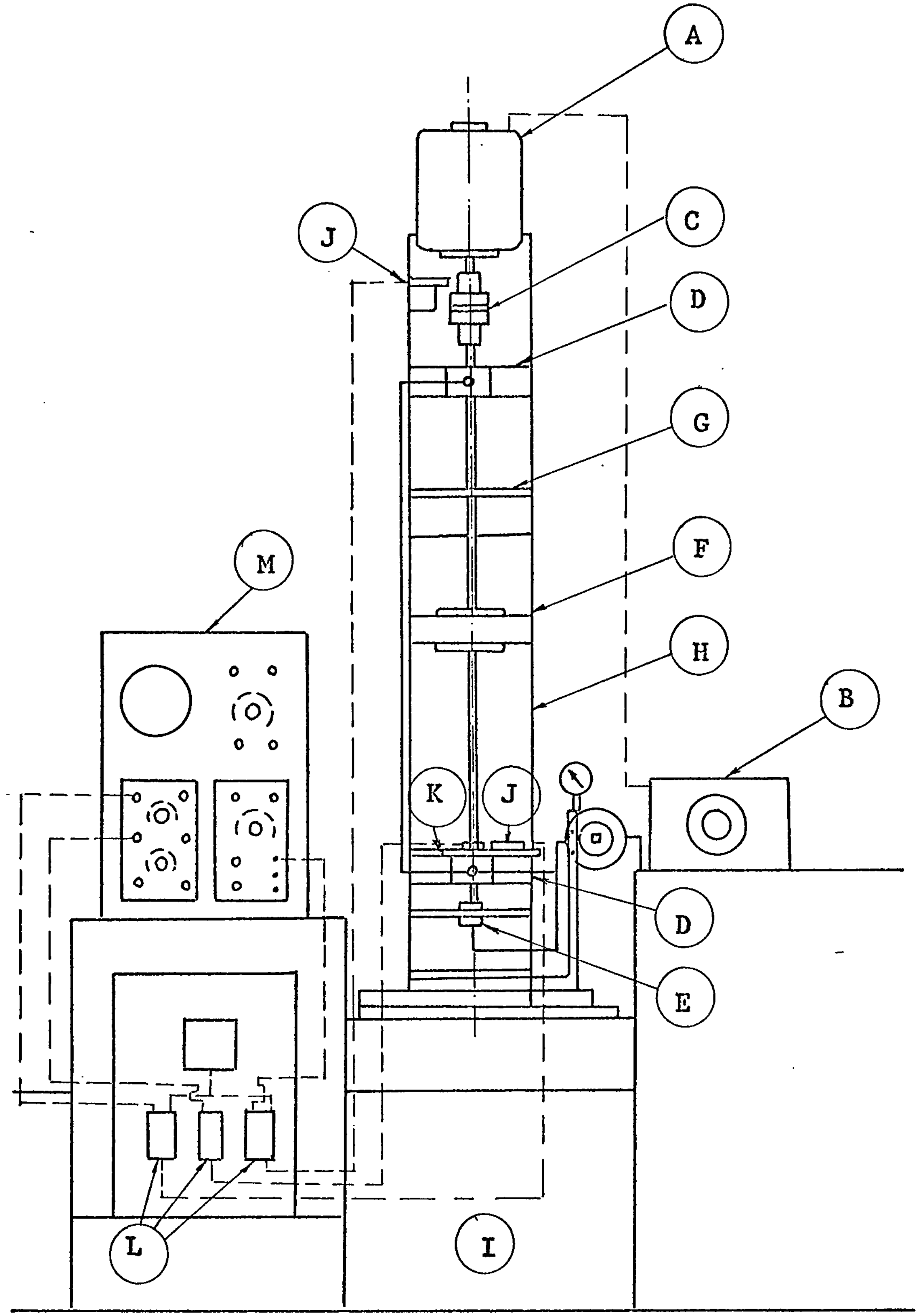

Fig. 5 Experimental Arrangement

CHAPTER II

DESCRIPTION OF APPRATUS AND INSTRUMENTATION

A. Apparatus

General The shaft materials used in the investigation were SAE 1018 steel, ASTM 2017 aluminum alloy, and a copper-manganese alloy containing 18% copper-82% manganese. These precise specifications are given in Table 1.

Construction In Fig. 5 the general arrangement of the equipment is shown. The motor (A) was a 1/4-hp compound-control constant-torque D. C. machine. The drive shaft was coupled to the experimental shaft by a flexible coupling (C). All of the experimental shafts were 30-1/2 inches long and 1/2 inch in diameter. Details of the air bearings are shown in Fig. 6.

As can be seen in Fig. 5. each experimental shaft was provided with a 3-in. diameter, 2.53-lb. balanced disk located at its midpoint. Provision was made to introduced an unbalance of 1.35×10^{-3} lb-in which is equivalent to a center-of- gravity displacement $\rho = 533 \mu m$.

In the interest of safety, guards (F and G) were provided. These guards were also used as supports upon which the motion-measuring instruments were mounted

The rotating system and its supports were set on a heavy post (H) and mounted on an isolated elastic foundation (I)

Table 1

Specification of the Materials

Properties \ Materials	Steel	Copper-Manganese	Aluminum Alloy
Density	0.288 lb/in^3	0.264 lb/in^3	0.101 lb/in^3
Young's Modulus	30×10^6 psi	13×10^6 psi	10.5×10^6 psi
Damping Capacity at Low Stress Percent		7	
Tensile Stress	64×10^3 psi	68×10^3 psi	
Proportional Limit	54×10^3 psi	24×10^3 psi	12×10^3 psi

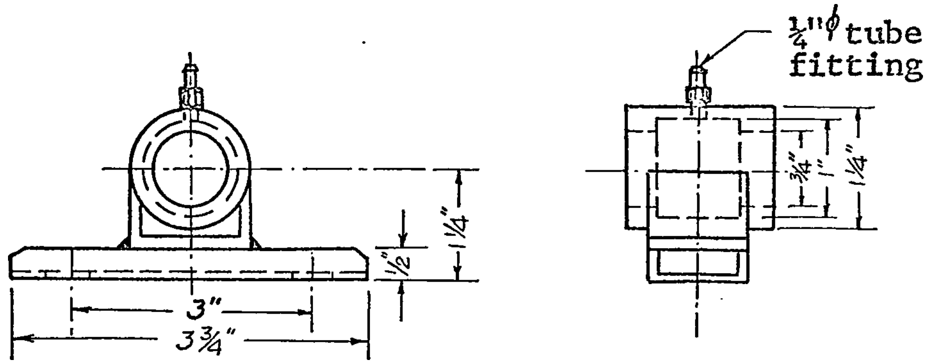

(a) Pillow Block

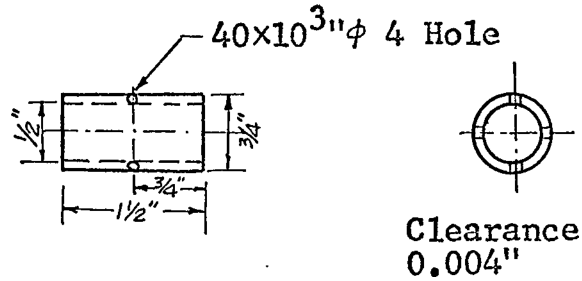

(b) Bushing

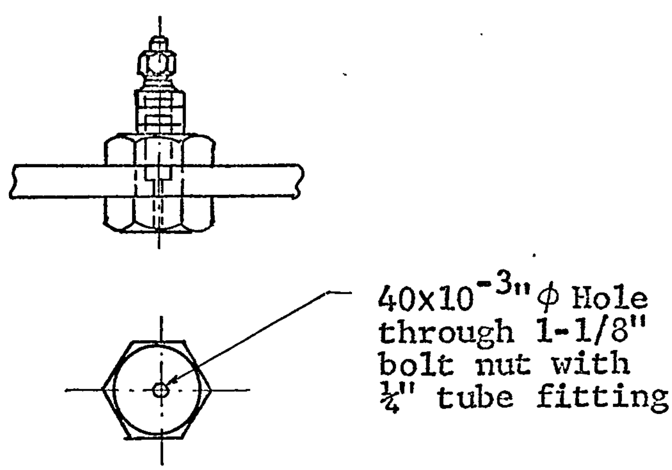

(c) Thrust Bearing

Fig. 6 Air Bearings

(Fig. 5) in order to isolate the foundation.

B. Instrumentation

In Fig. 7 a block diagram of the instrumention is shown. Two Bentley Nevada 3000 Series inductive probes (J) were used to measure the motion of the shaft during rotation. They were attached to the guard block (K) along perpendicular axes. Another identical was mounted near the driving shaft; it was used as a revolution counter and angular position reference.

The signals, which are proportional to the change in the air gap between the probes and the shaft surface, were transmitted to the Bentley Nevada 3000 Series proximitors (L) and thence to the Tektronix 561A four-trace Oscilloscope (M). A Hewlett Packard 196A oscilloscope camera was used to record the motion and timing traces.

A depth micrometer and a feeler gage were also used to measure the initial runout of the shaft.

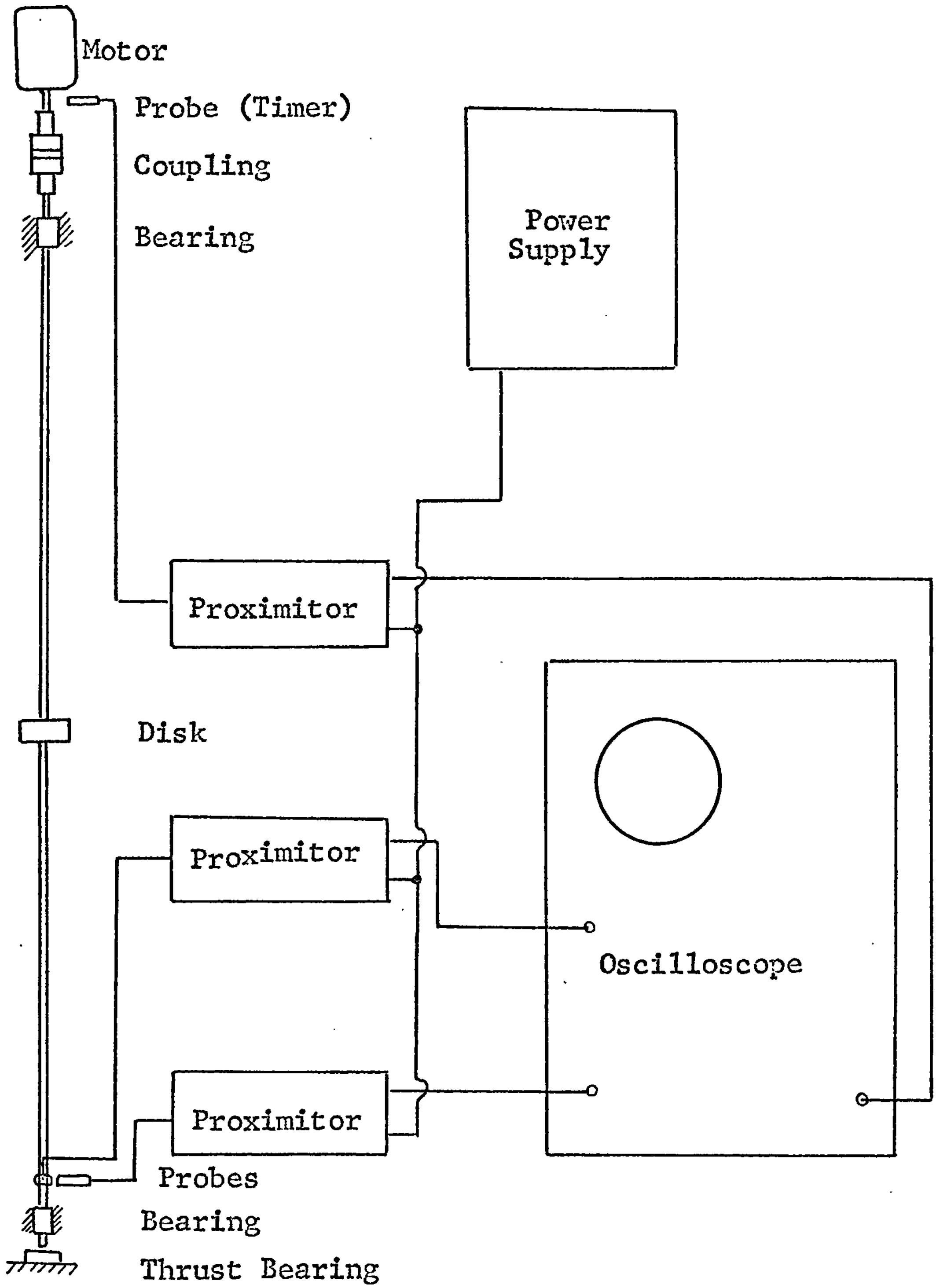

Fig. 7 Block Diagram of Instrumentation

CHAPTER III

TEST PROCEDURES

In order to study the role and effect of damping on the response of a flexible shaft in the region of a critical speed, the following factors were taken into account

1. Shaft material.
2. Bearing type.
3. Shaft-disk configuration.

The details of the experimental are given in Table 2.

In this study, three different shaft materials were used. Each shaft-disk configuration was subjected to the same series of test. Air bearings, self-aligning ball bearings and oil-film sleeve journal bearings were used with each shaft.

When the shaft rotates, its motion at the measuring point is a function of both initial runout and the unbalance present in the rotor. Therefore, in order to determine the runout, it is necessary to rotate the shaft by hand and measure its distance from a fixed point. From this information, the relationship between the magnitude and angular position of the runout relative to the timer position on the shaft can be plotted. The results of such measurements on the three test shafts in 30-degree steps is shown in Fig. 8, 9, and 10.

The shaft is rotated from zero speed to a speed above the critical speed. The once-per-revolution response is

Table 2

Details of Shafts Used in Test

(Each ½-in. dia. and 27¼-in. between bearings and a 2.53 lb. weight in center)

Shaft Identification Letter	Material of Shaft	Bearings	Critical Speed (measured) rpm
A	steel	self-aligning ball bearing	1700*
B	cu-mn	"	1100*
C	Al-alloy	"	1000*
D	steel	journal bearing	2475
E	cu-mn	"	1720
F	Al-alloy	"	1650
G	steel	air bearing	2580
H	cu-mn	"	2000
I	Al-alloy	"	1945

* Note: For this case, the shaft behaves essentially as a center-mass-loaded, simply supported beam and the caputed natural frequencies (critical speeds) are 1740, 1145, and 1030 rpm, respectively, for steel, copper-manganese, and aluminum alloy shaft. For other bearing conditions the system is stiffened and the critical speeds are higher.

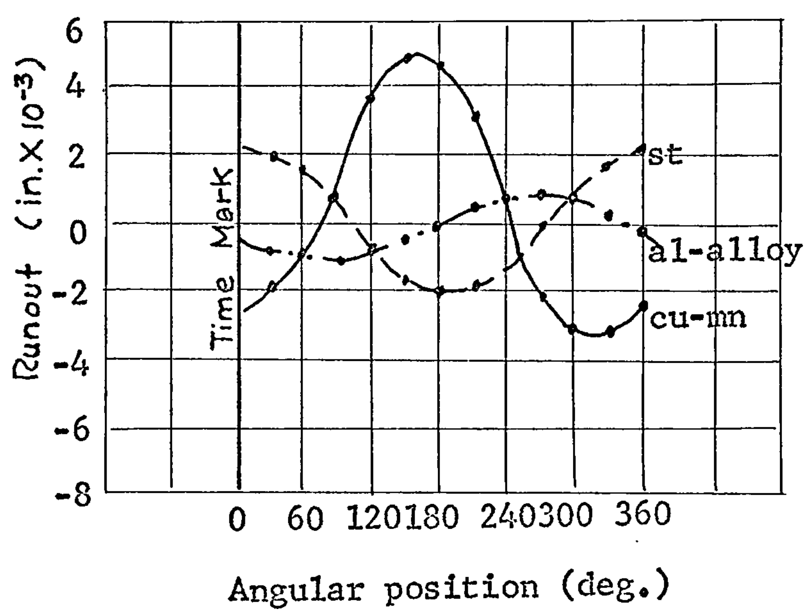

Fig. 8 Initial Runout of the Shafts in Self-aligning Ball Bearings

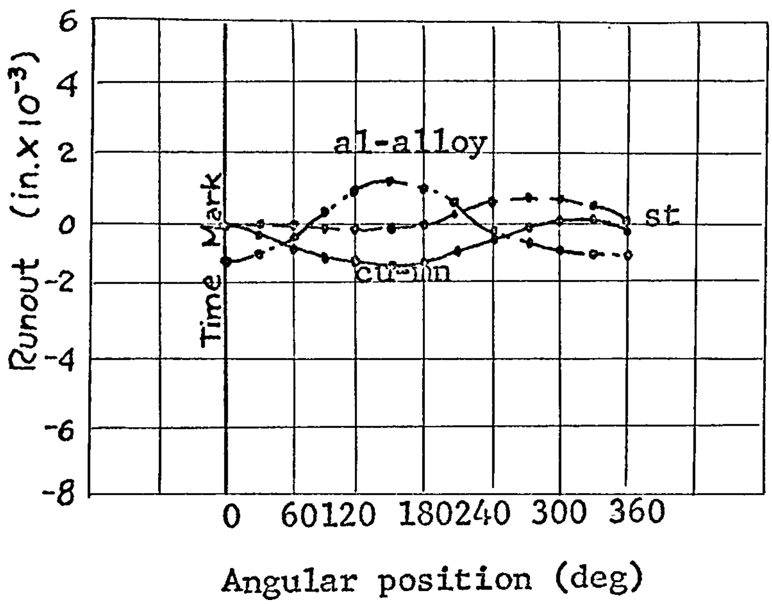

Fig. 9 Initial Runout of Copper-Manganese Shaft in Journal Bearings

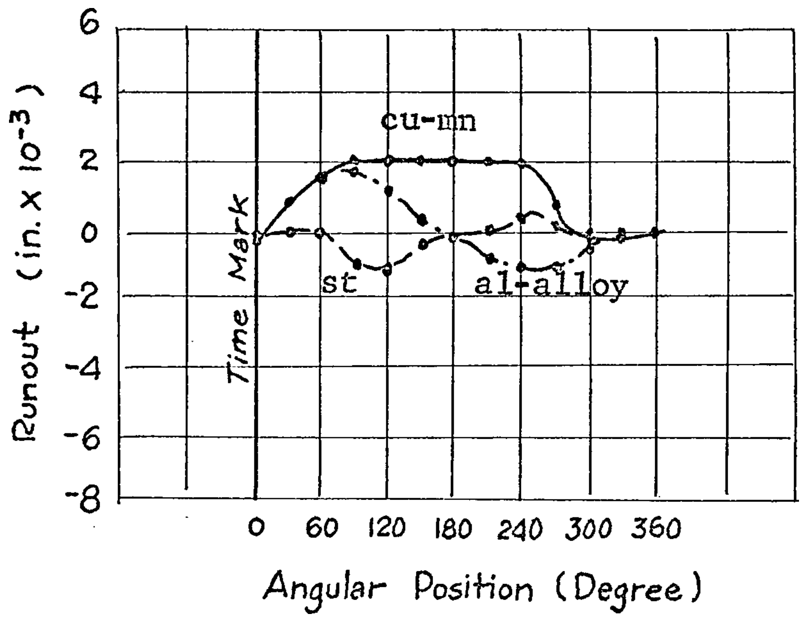

Fig. 10 Initial Runout of Shafts in Air Bearings

measured and related (by means of the timer signal) to the angular position of the shaft. These results (for the various shaft materials and bearing conditions) are shown in Figs. 11-20.

The magnitude and angular position of the rotating response may be found by plotting the vector difference of the static and running displacements at the measuring positions. This yields the net response which can be attributed to the inherent unbalance only and, thus, the effect of initial runout is eliminated. These results are given in Tables 3-5

When the two perpendicular probes, used to measure the displacement of the driven shaft, are connected to the x and y axes of the ocsilloscope, a Lissajous figure is obtained. Examples of this are shown in Fig. 21.

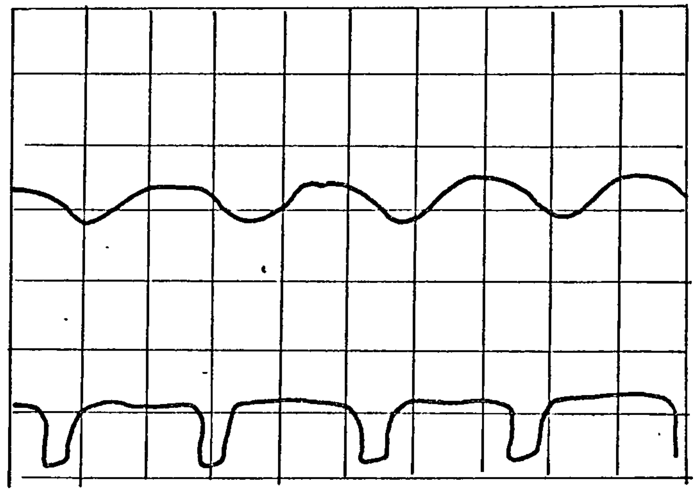

(a) rpm = 1250

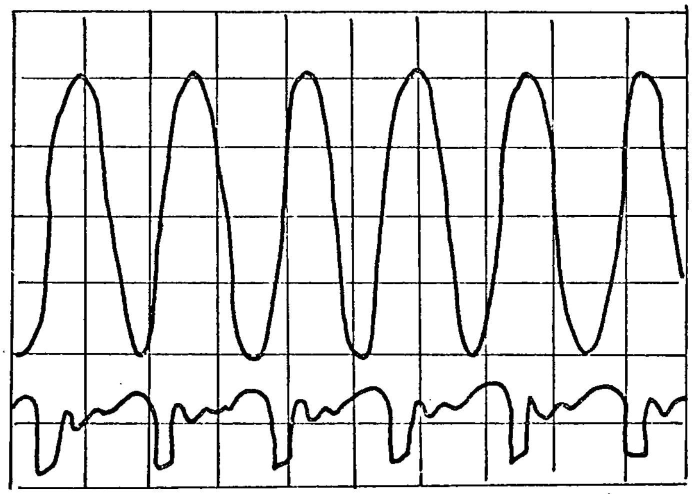

(b) rpm = 1765

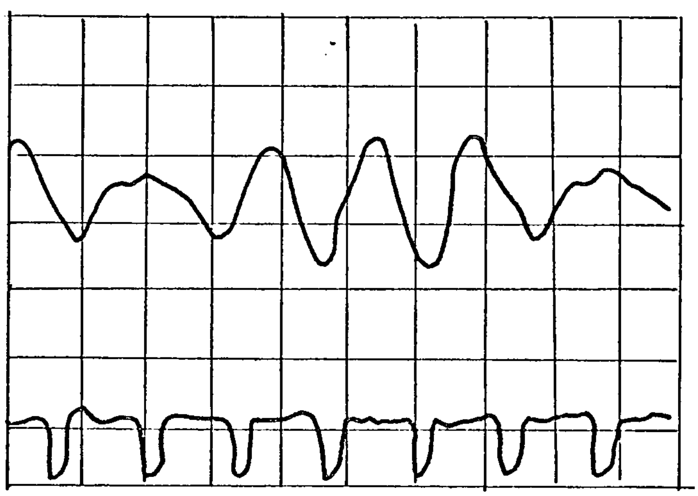

(c) rpm = 2140

Fig. 11 Displacement of Steel Shaft in Self-aligning Ball Bearings

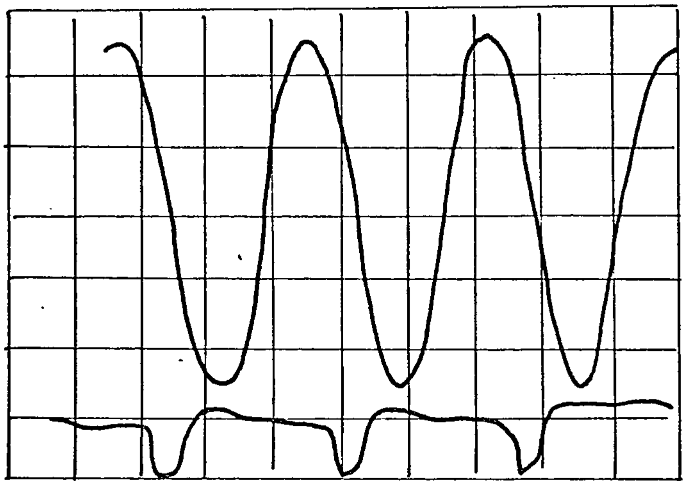

(a) rpm = 1100

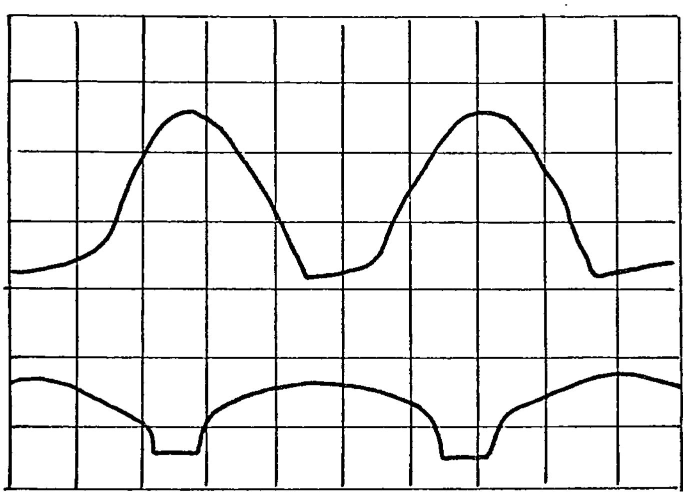

(b) rpm = 1365

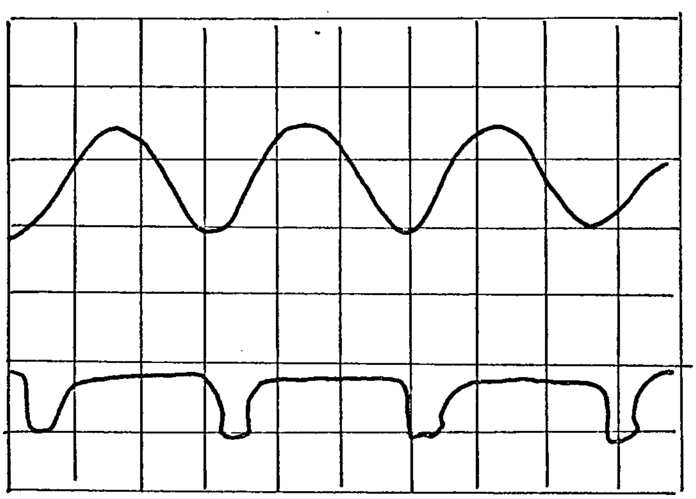

(c) rpm = 2072

Fig. 12 Displacement of Cu-mn Shaft in Self-aligning Ball Bearings

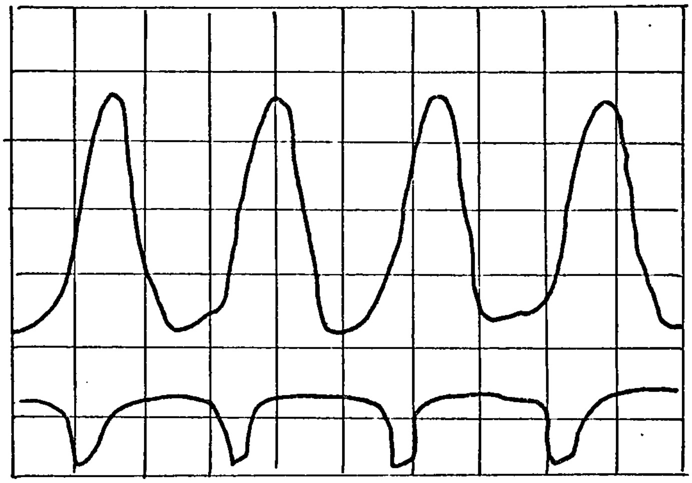

(a) rpm = 1300

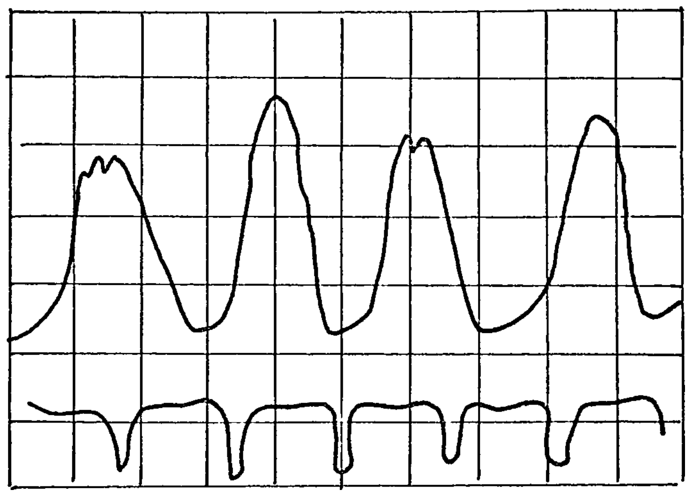

(b) rpm = 1875

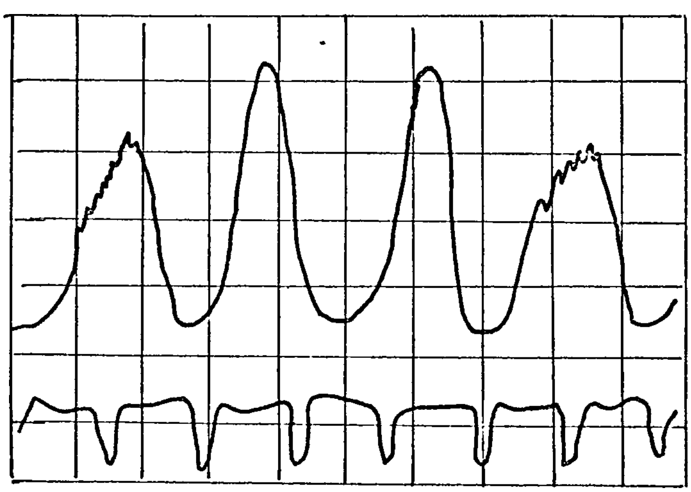

(c) rpm = 2140

Fig. 13 Displacement of Al-alloy Shaft in Self-aligning Ball Bearings

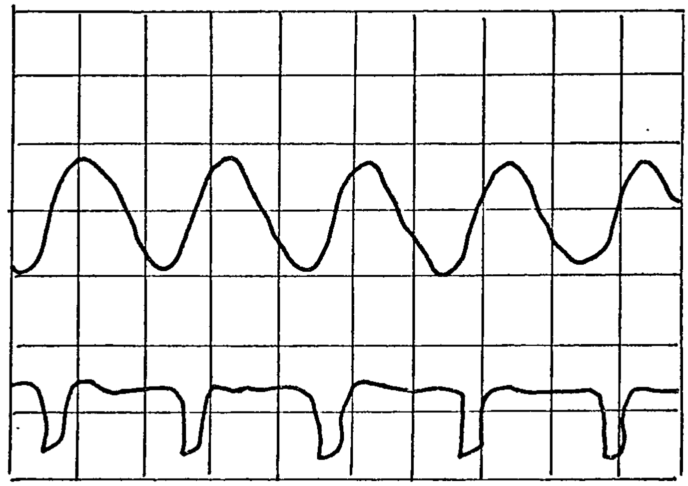

(a) $\omega < \omega_n$

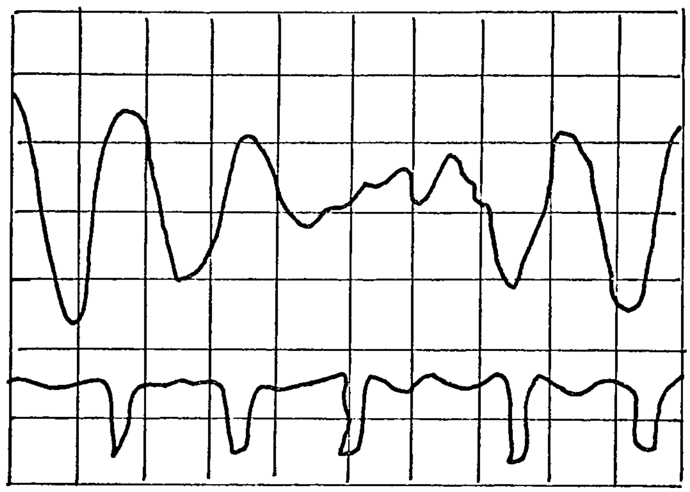

(b) $\omega = \omega_n$

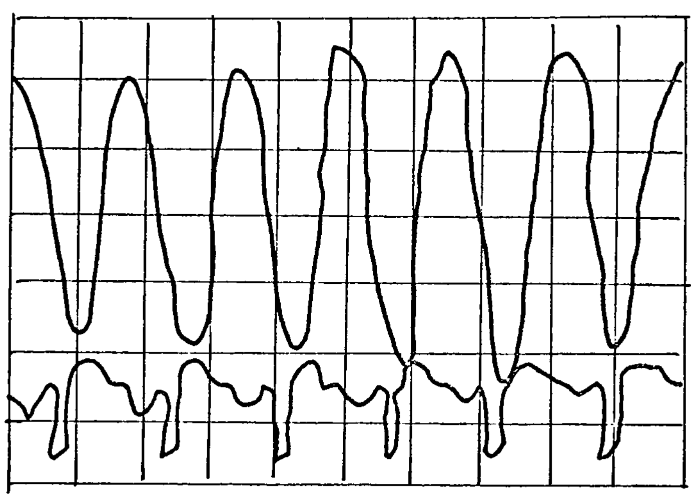

(c) $\omega > \omega_n$

Fig. 14 Displacement of Cu-mn Shaft in Journal Bearings
Time base scale 20ms/Div, Voltage 1volt/Div.

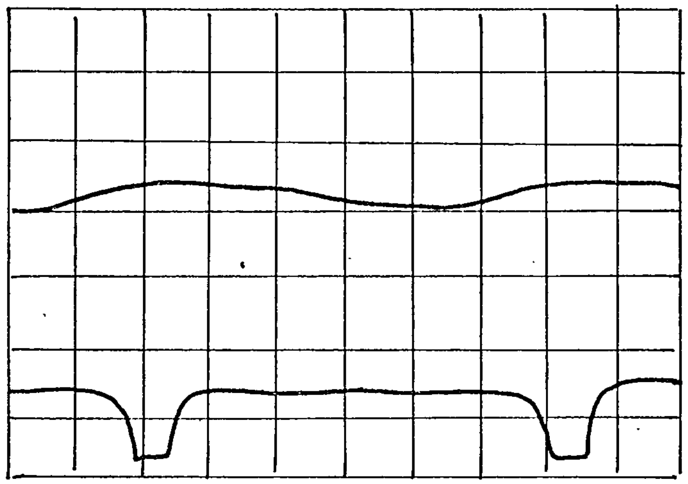

(a) rpm = 955

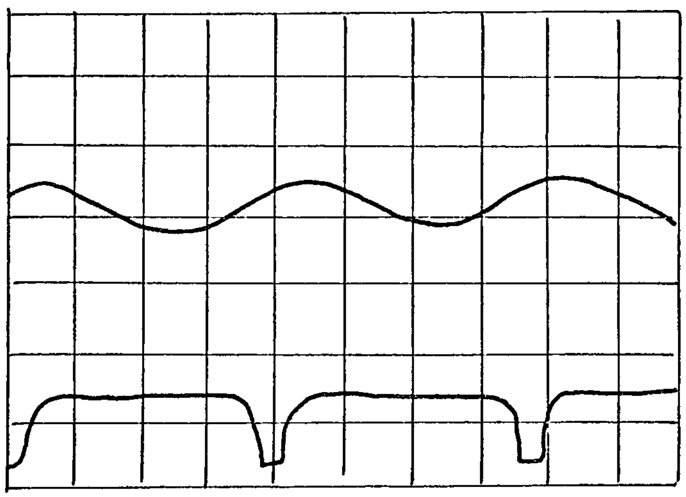

(b) rpm = 1540

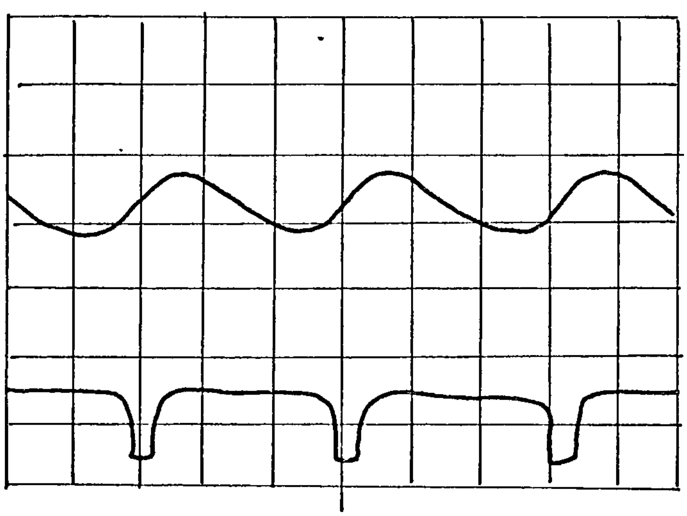

(c) rpm = 1900

Fig. 15 Displacement of Steel Shaft in Air Bearings
Time base 10 ms/Div, Voltage 1 volt/Div

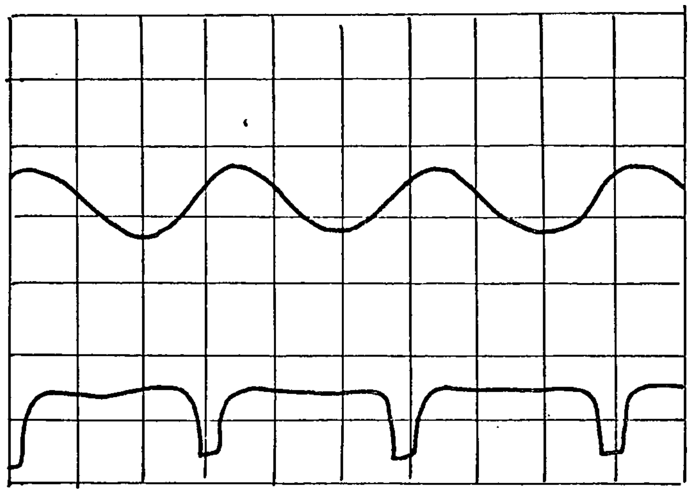

(d) rpm = 2000

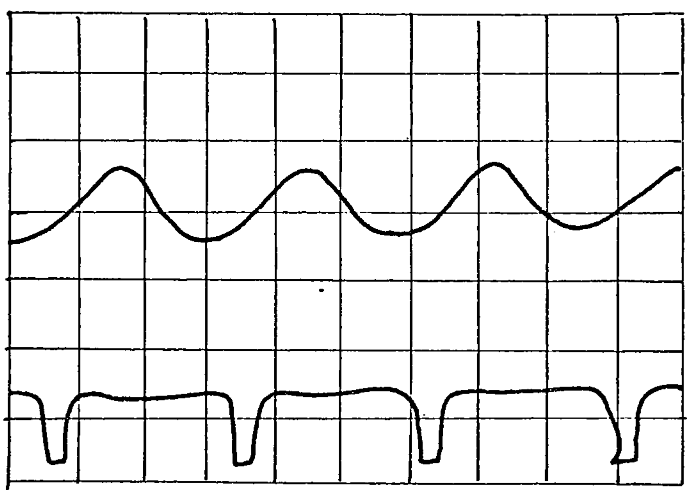

(e) rpm = 2140

Fig. 16 Displacemant of Steel Shaft in Air Bearings
Time base 10 ms/Div, Voltage 1 volt/Div.

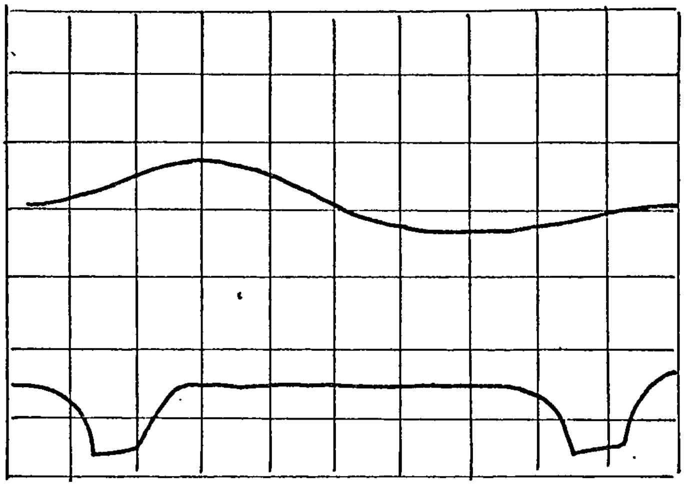

(a) rpm = 834

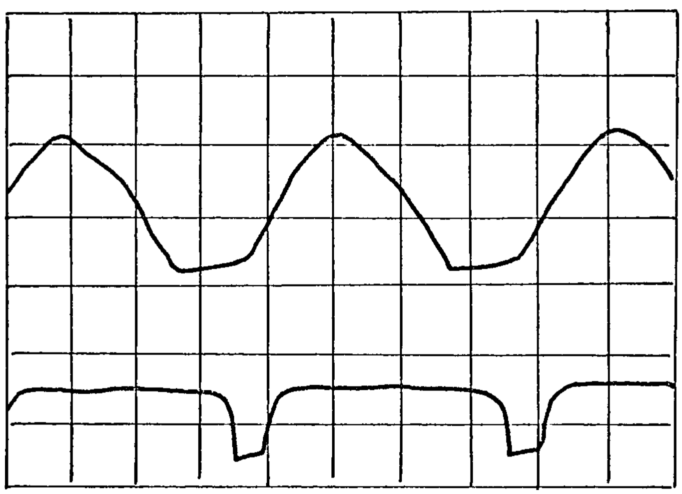

(b) rpm = 1430

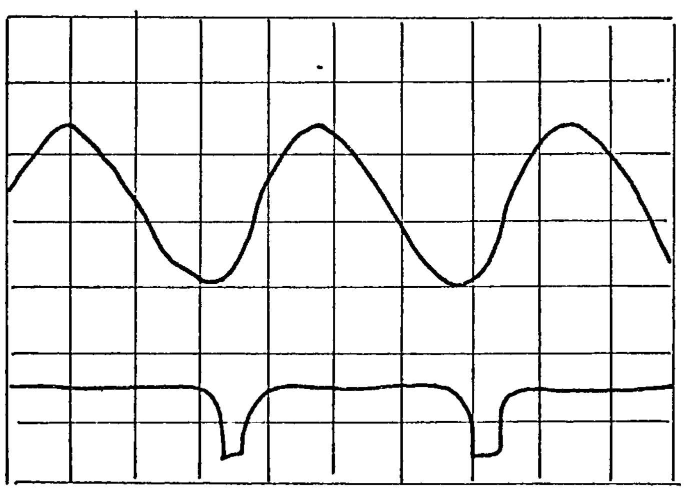

(c) rpm = 1600

Fig. 17 Displacement of Cu-mn Shaft in Air Bearings
Time base 10 ms/Div, Voltage 1 volt/Div.

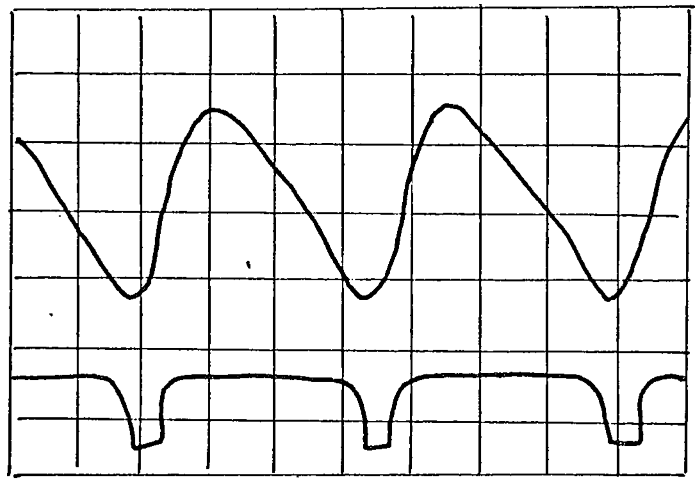

(d) rpm =1730

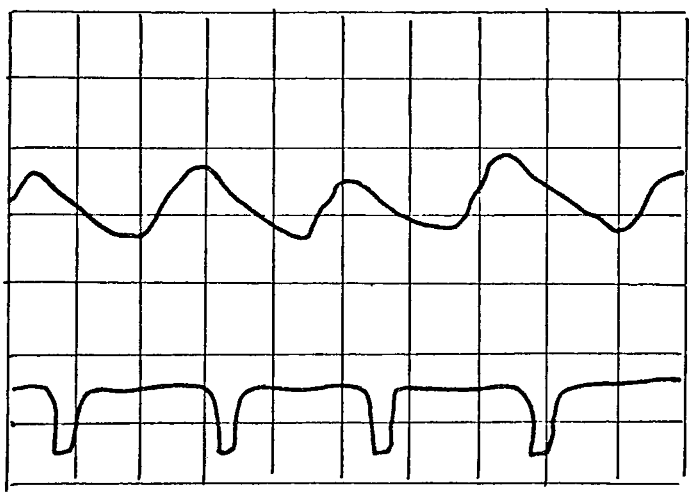

(e) rpm =2610

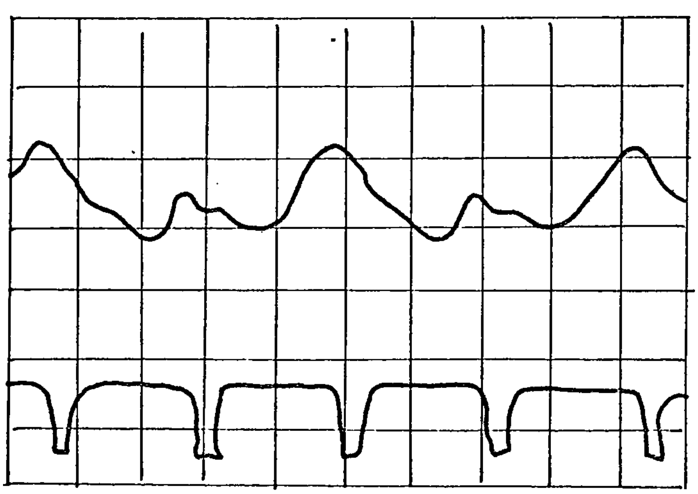

(f) rpm = 2730

Fig. 18 Displacement of Cu-mn Shaft in Air Bearings
Time base 10 ms/Div, Voltage 1 volt/Div.

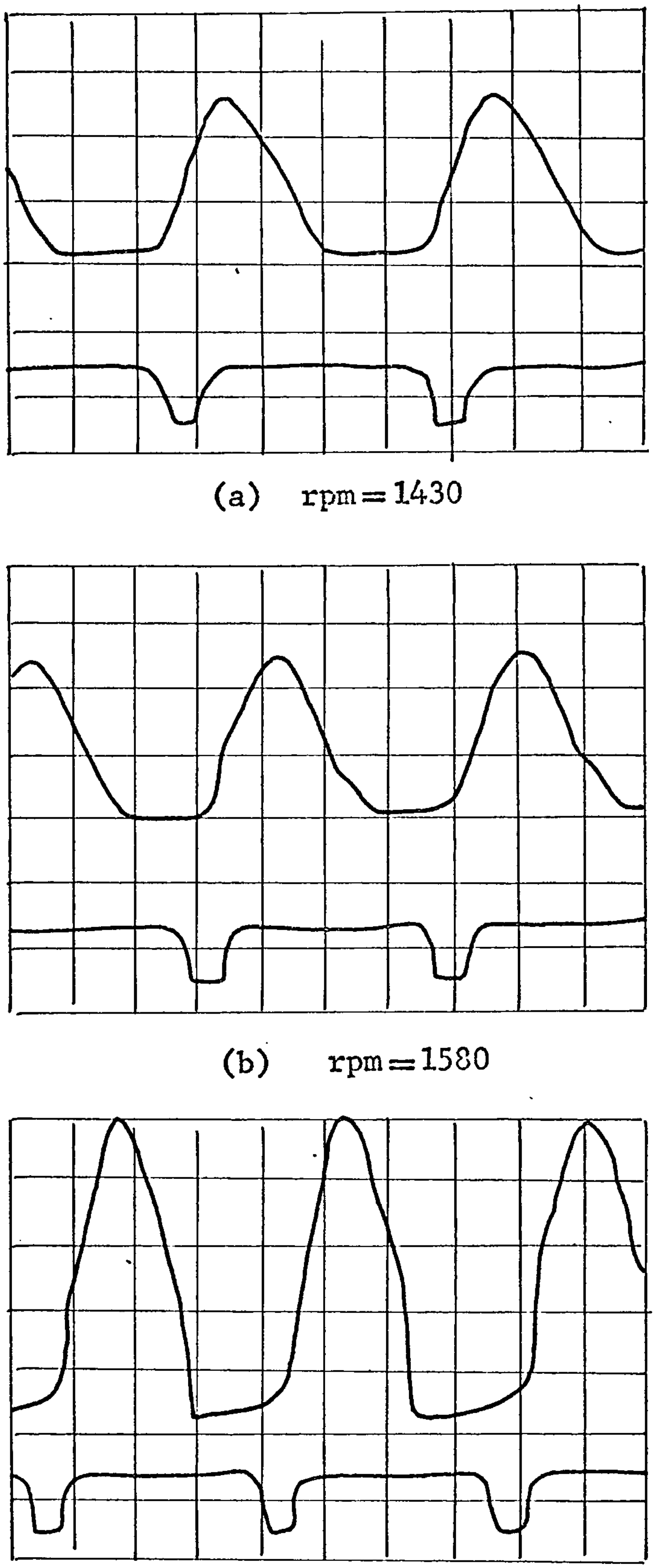

(a) rpm = 1430

(b) rpm = 1580

(c) rpm = 1645

Fig. 19 Displacement of Al-alloy Shaft in Air Bearings
Time base 10 ms/Div, Voltage 2 volt/Div

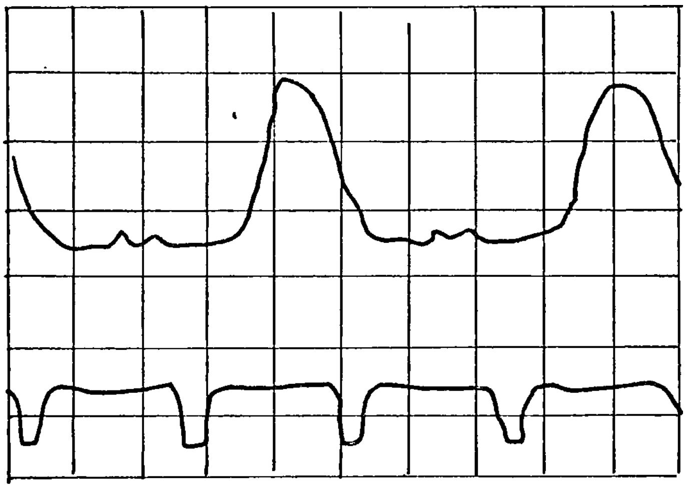

(d) rpm=2500

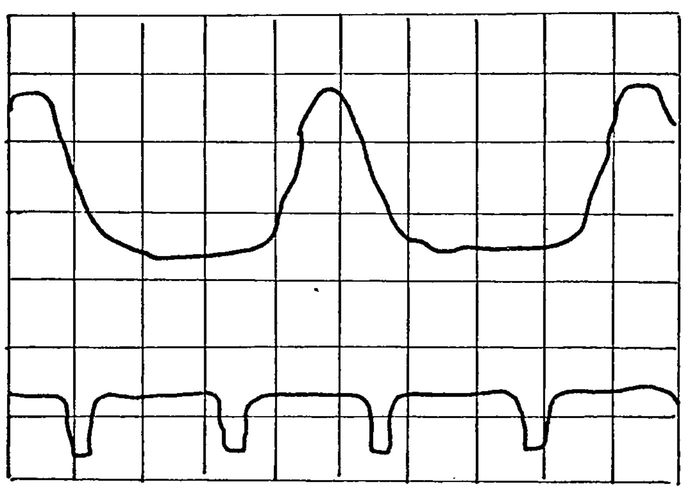

(e) rpm=2670

Fig. 20 Displacement of Al-alloy Shaft in Air Bearings
Time base 10 ms/Div, Voltage 2 volt/Div

Table 3

The Displacements of the Shafts in Ball Bearings

Speed		Steel Shaft			Copper Manganese Shaft			Aluminum Alloy Shaft		
rpm	rad/sec	ω/ω_n	A_R comp	A_R meas	ω/ω_n	A_R comp	A_R meas	ω/ω_n	A_R comp	A_R meas
334	35							0.32	1.11	1.1
600	62.8				0.52	1.29	1.13			
734	76.7							0.71	1.83	1.25
780	81.6	0.45	1.25	1.09						
1000	104.8							0.97	3.12	1.5
1016	106.4							0.98	3.11	1.59
1030	108							1.0	3.07	1.56
1110	116				0.97	3.44	1.77			
1145	120				1.0	3.42	1.75			
1250	131	0.72	1.94	1.39						
1300	136							1.26	1.39	1.36
1365	143				1.19	1.83	1.65			
1700	178	0.98	5.16	2152						
1740	182	1.0	5.19	2.47						
1765	185	1.03	5.16	2.3						
1925	201.5									
2072	216.5				1.81	0.43	1.48			
2140	224	1.26	1.58	1.65						
ω_n		182			120			108		

Table 4

The Displacements of the Shafts
in oil-film journal bearings

Speed		Steel Shaft			Copper Manganese Shaft			Aluminum Alloy Shaft		
rpm	rad/sec	ω/ω_n	A_R comp.	A_R meas.	ω/ω_n	A_R comp.	A_R meas.	ω/ω_n	A_R comp.	A_R meas.
326	34.1	0.13	1.02	1.01						
396	41.5				0.23	1.05	1			
715	75							0.42	1.23	1.21
883	92.5	0.35	1.13	1.13						
925	97				0.53	1.38	1.05			
1050	110							0.62	1.62	1.41
1430	150				0.82	2.82	1.11			
1500	157	0.6	1.49	1.15						
1580	165				0.9	4.29	1.22	0.93	5.3	1.51
1620	170				0.93	5.15	1.32			
1650	176				0.96	6.26	1.32	0.99	6.89	1.70
1685	177							1.0	6.84	1.64
1720	180				0.98	6.9	1.53			
1760	184				1.0	7.06	1.52	1.04	5.8	1.60
1765	184.5				1.02	7.04	1.26			
2140	224	0.82	2.62	1.35						
2475	259	0.99	3.33	1.73						
2515	263	1.0	10.1	1.69						
ω_n		263			184			177		

Table 5

The Displacements of the Shafts in Air Bearings

Speed		Steel Shaft			Copper Manganese Shaft			Aluminum Alloy Shaft		
rpm	rad/sec	ω/ω_n	A_R comp.	A_R meas.	ω/ω_n	A_R comp.	A_R meas.	ω/ω_n	A_R comp.	A_R meas.
834	87.2				0.41	1.2	1.05			
955	100	0.37	1.16	1.03						
970	103							0.49	1.13	1.21
1430	149.5				0.71	1.97	1.11	0.72	2.04	1.43
1540	161	0.6	1.54	1.1						
1580	165							0.79	2.58	1.45
1600	167.5				0.79	2.56	1.13			
1640	172							0.82	2.97	1.57
1670	174.5							0.84	3.18	1.55
1730	181				0.85	3.47	1.15			
1900	198.5	0.73	2.12	1.13						
1945	204							0.98	8.3	1.79
2000	209	0.77	2.42	1.15	0.99	8.70	1.24	1.	8.70	1.78
2030	212				1.	8.86	1.23			
2140	224	0.83	3.05	1.16						
2580	270	0.99	11.3	1.33						
2600	272	1.	11.4	1.31						
2610	274				1.29	1.48	1.07			
2730	285	1.05	7.35	1.17						
ω_n		272			212			209		

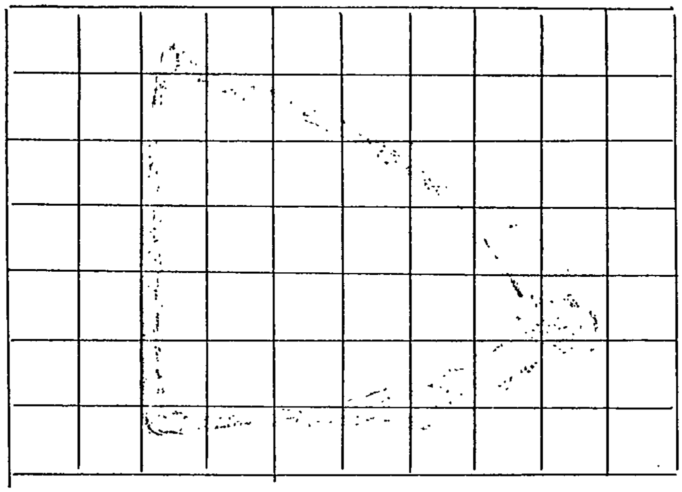

(a) $\omega < \omega_n$

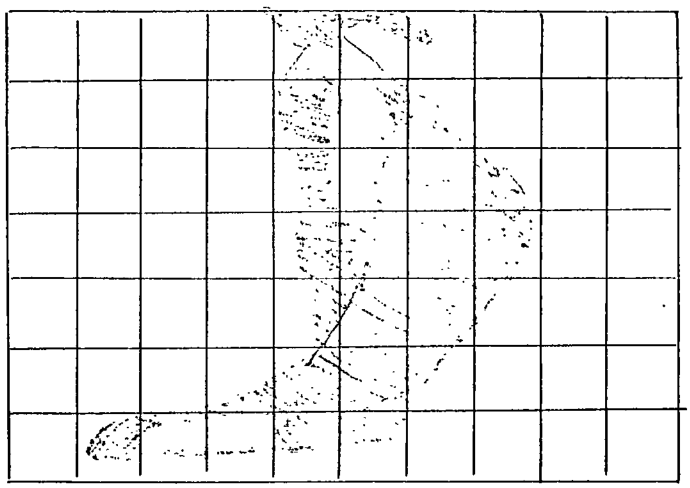

(b) $\omega = \omega_n$

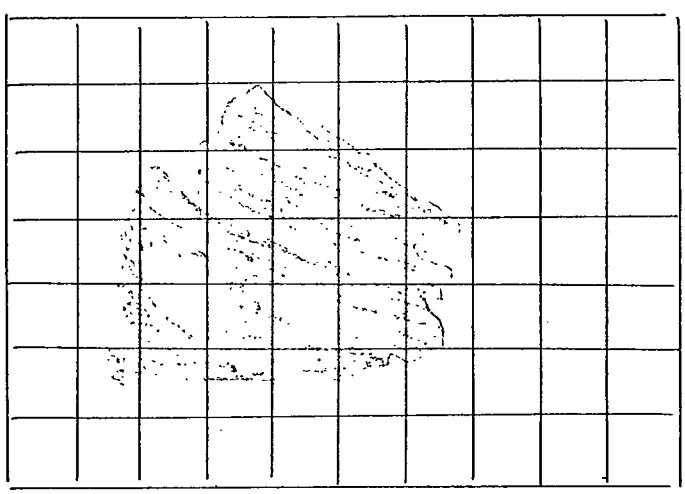

(c) $\omega > \omega_n$

Fig. 21 Lissajous Figure of the Rotating Shaft (Al-alloy)

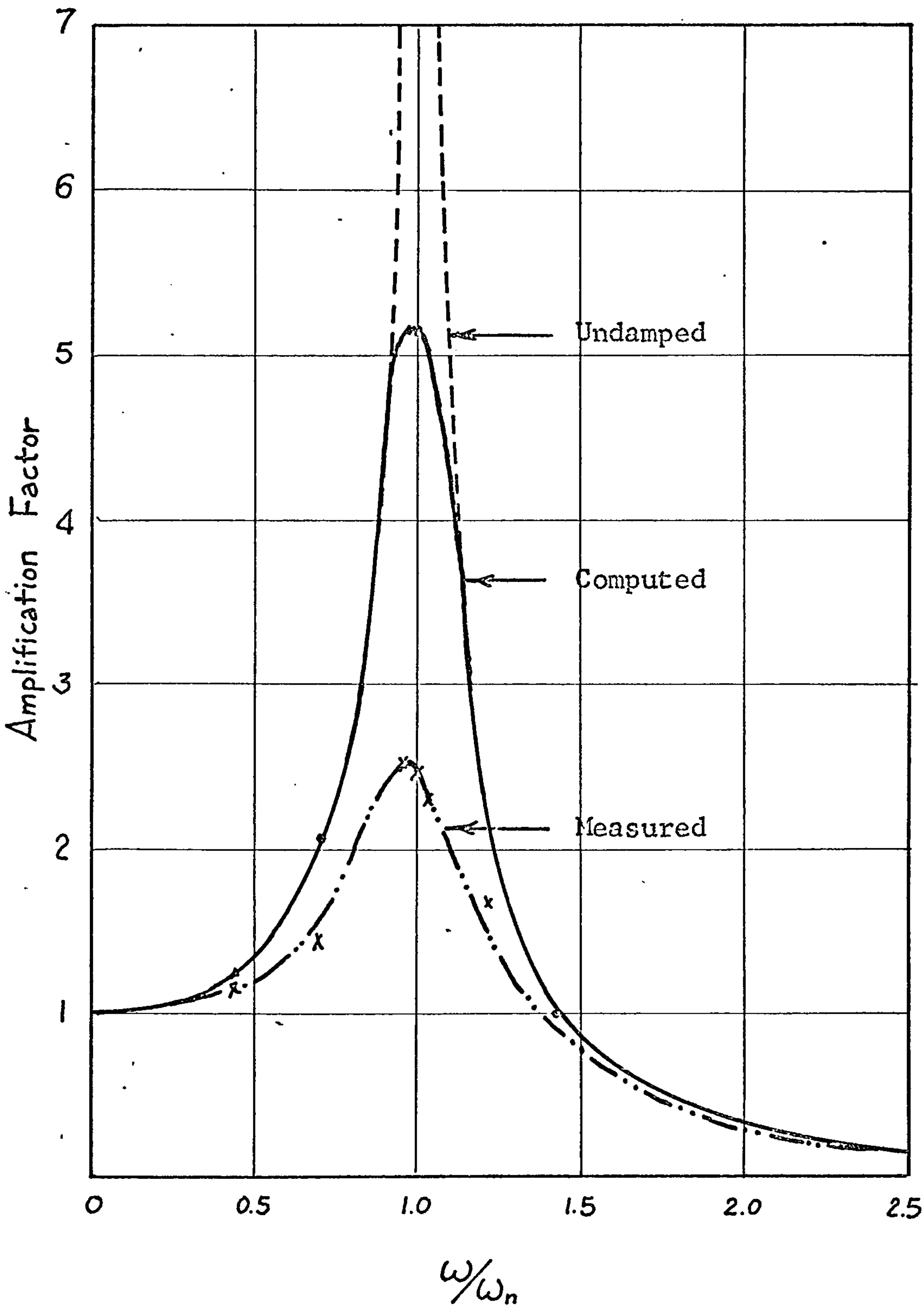

Fig. 22 Response of Steel Shaft in Self-aligning Ball Bearings

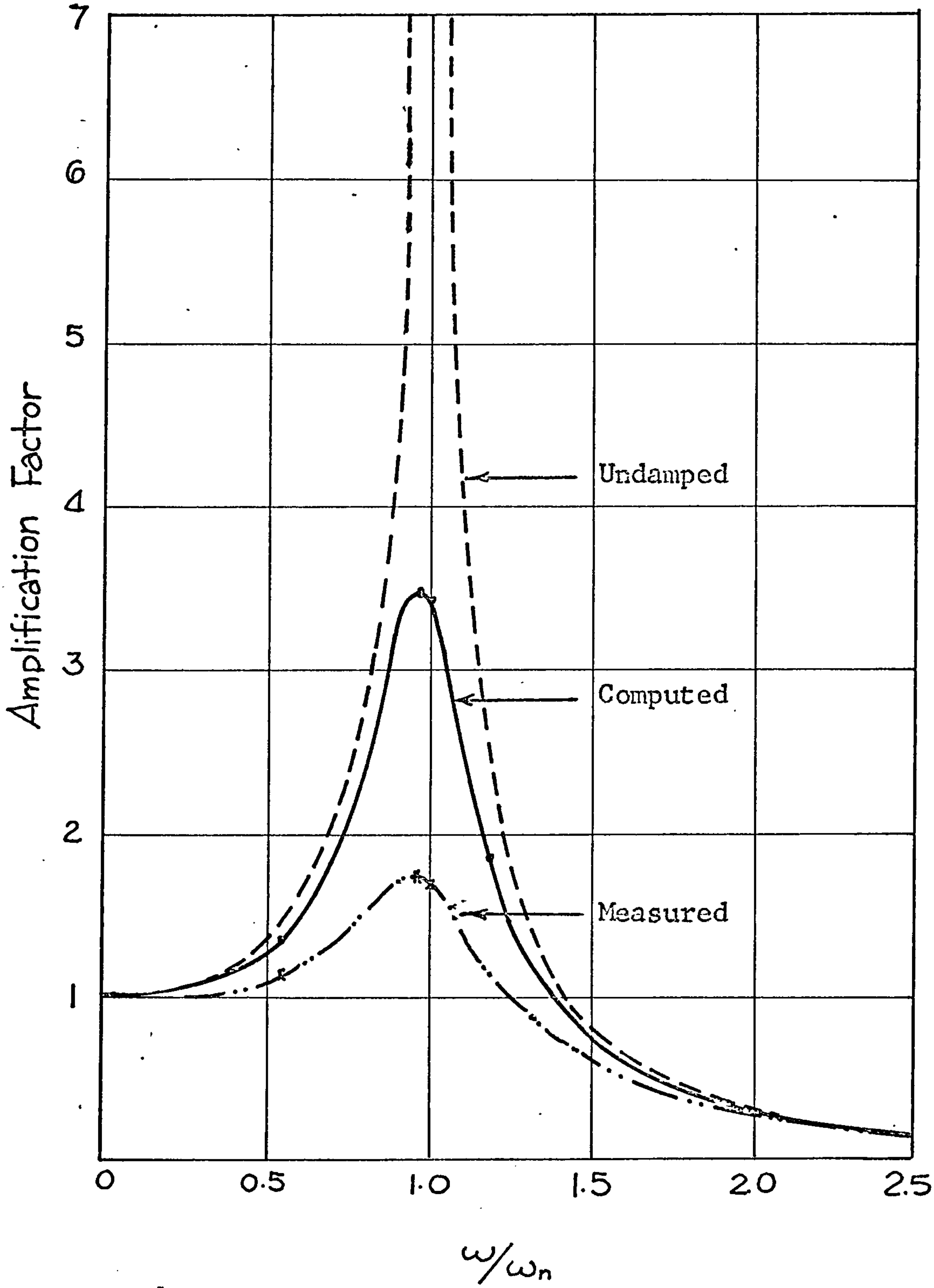

Fig. 23 Response of Copper-Manganese Shaft in Self-aligning Ball Bearings

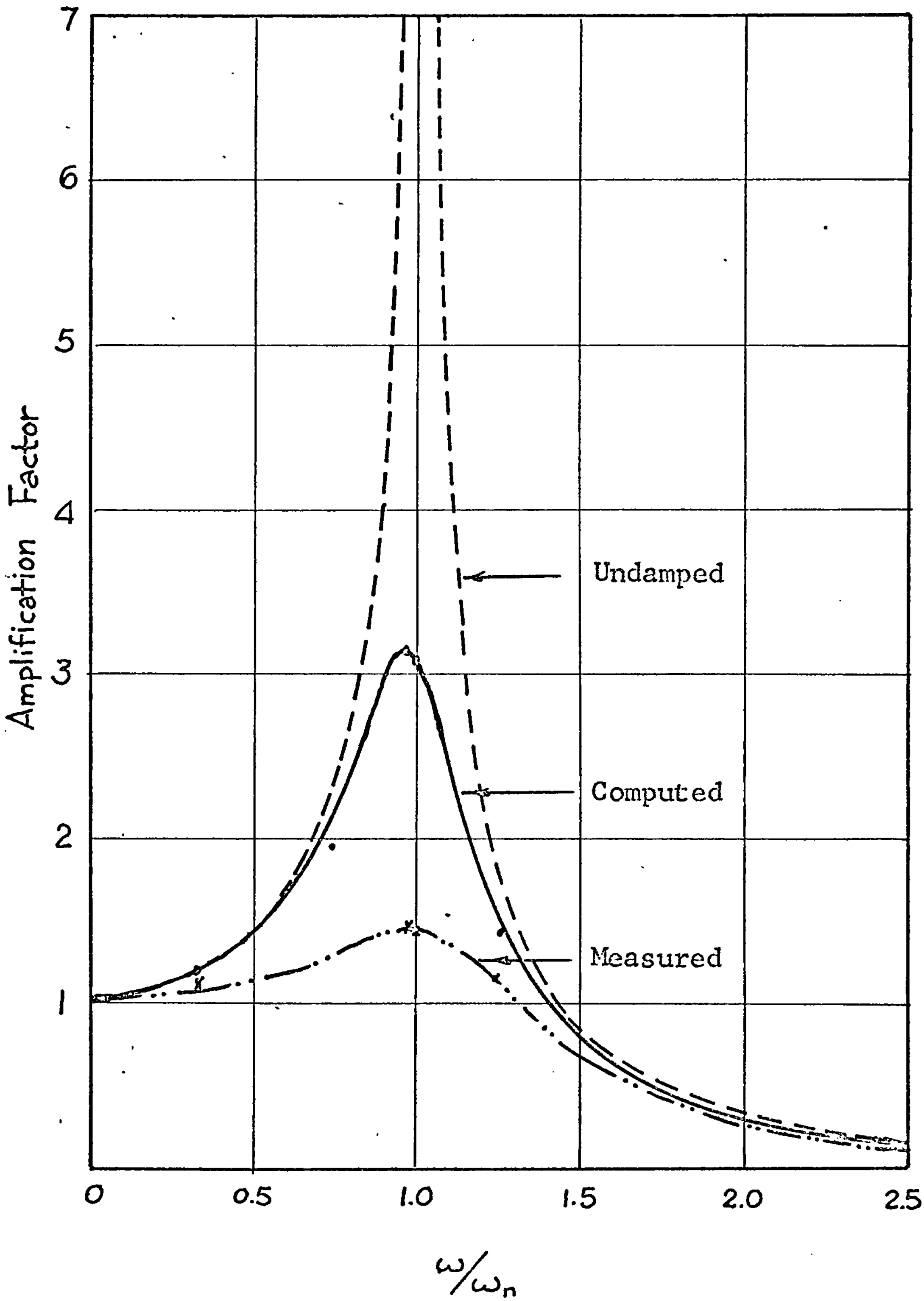

Fig. 24 Response of Aluminum-Alloy Shaft in Self-aligning Ball Bearings

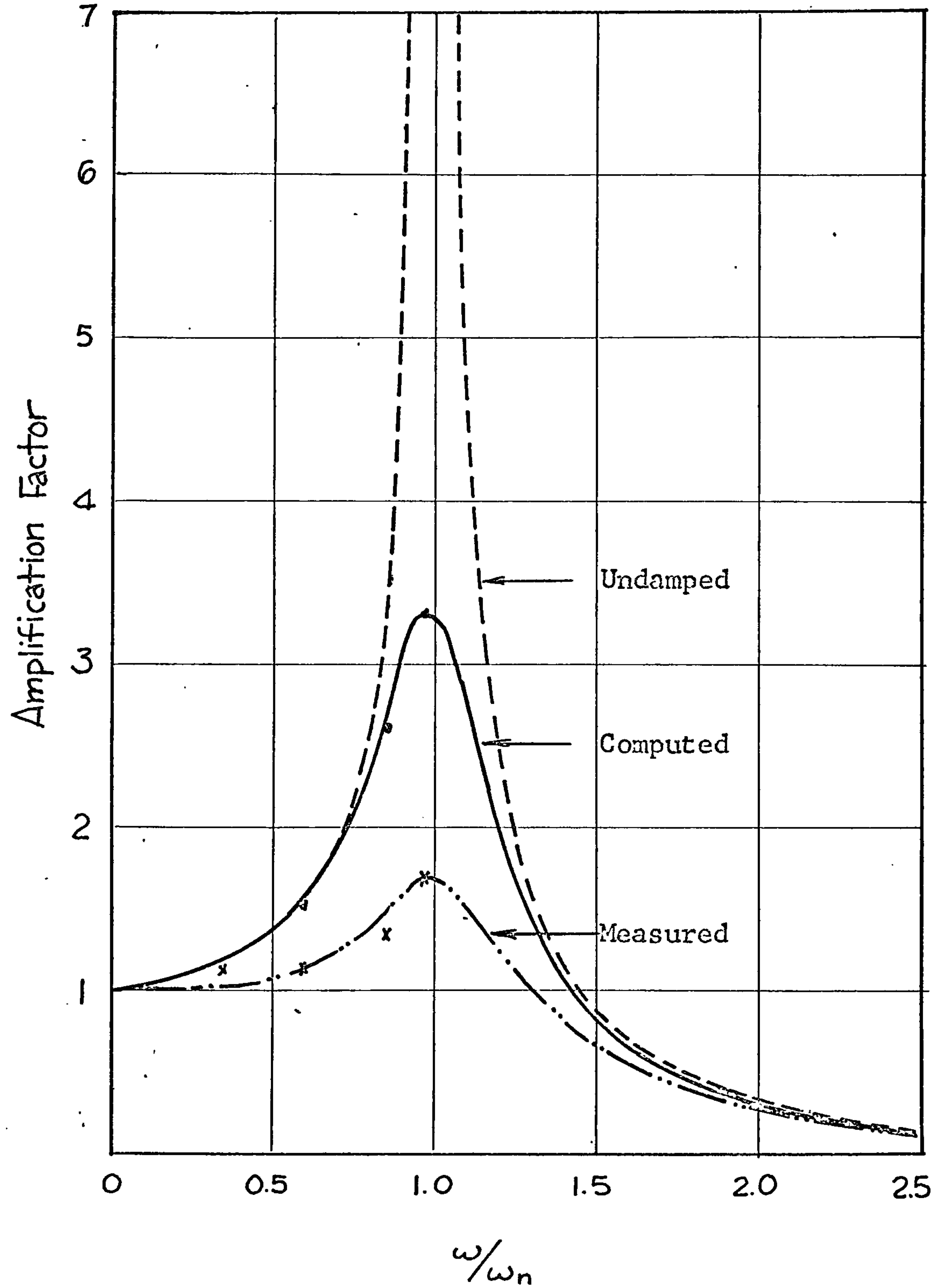

Fig. 25 Response of Steel Shaft in Oil-Film Journal Bearings

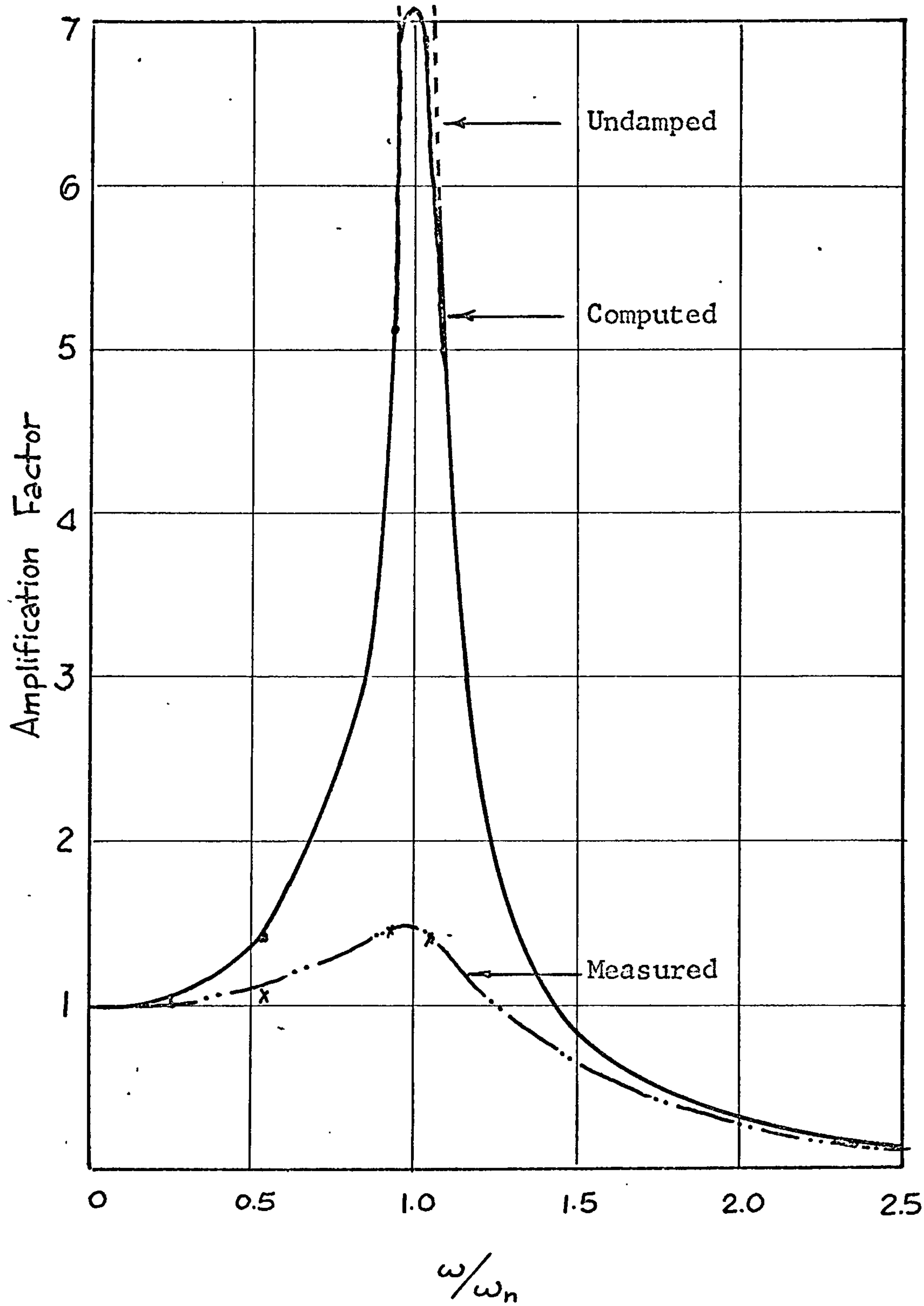

Fig. 26 Response of Copper-Manganese Shaft in Oil-Film Journal Bearings

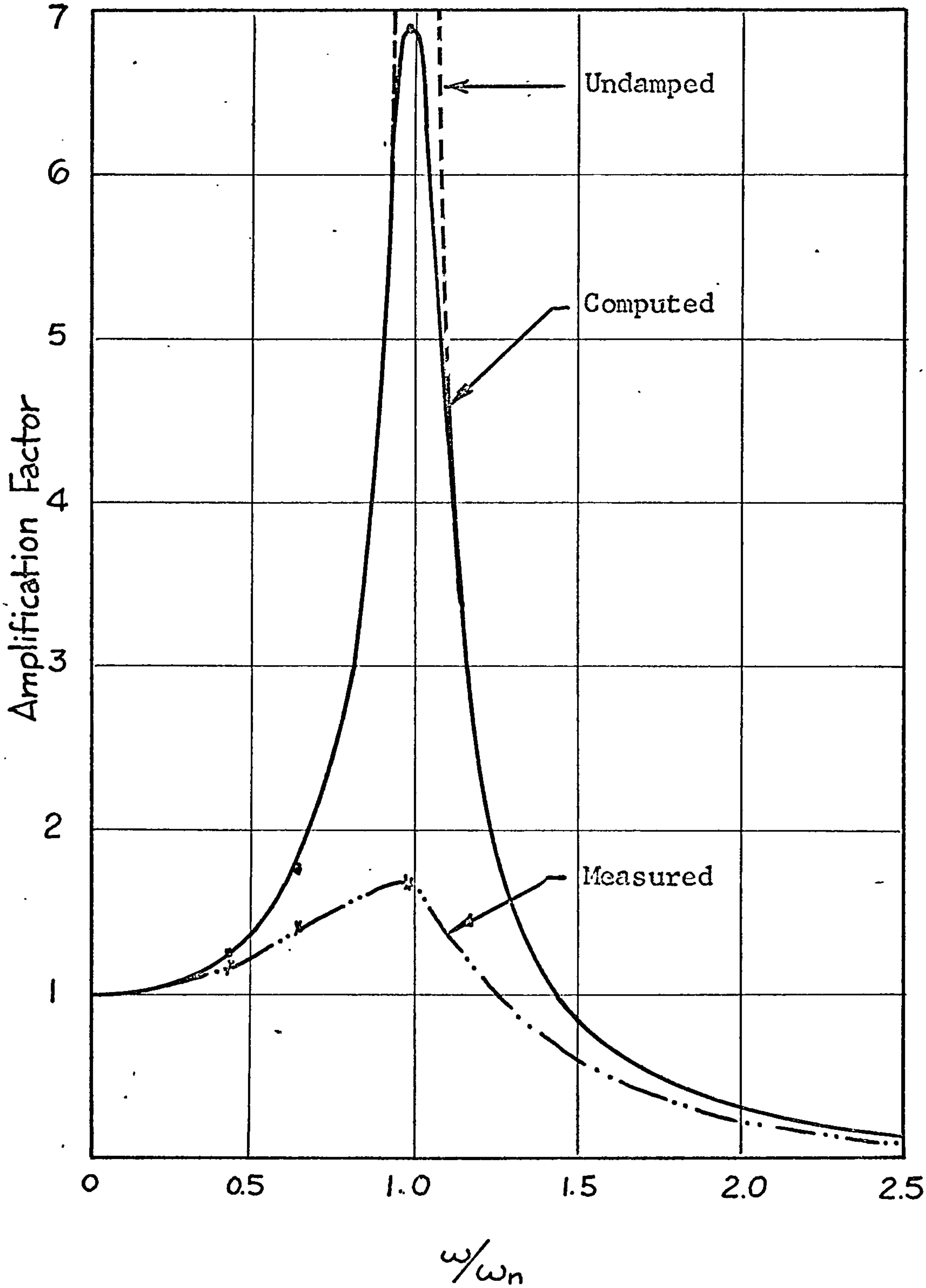

Fig. 27 Response of Aluminum-Alloy in Oil-Film Journal Bearings

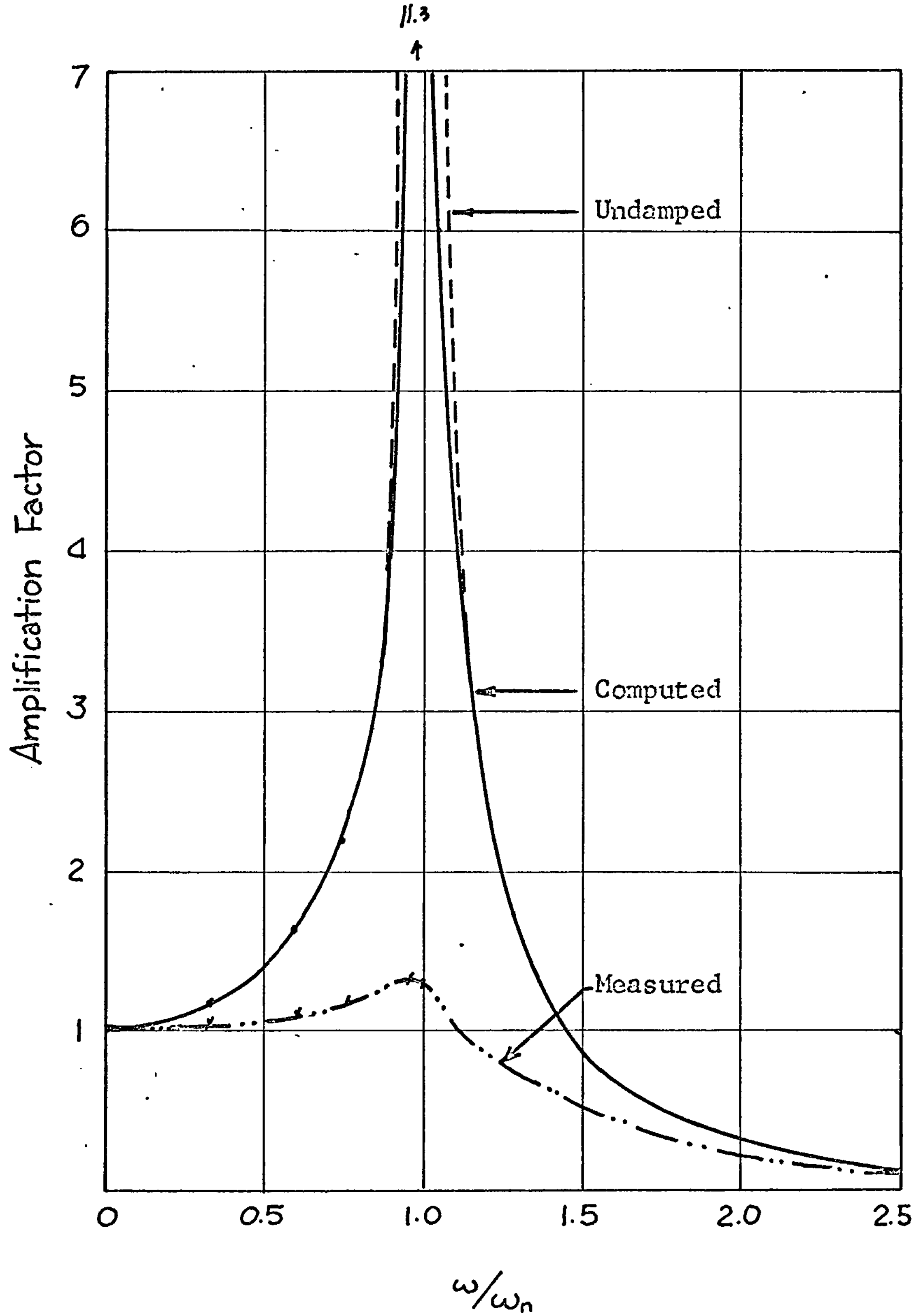

Fig. 28 Response of Steel Shaft in Air Bearings

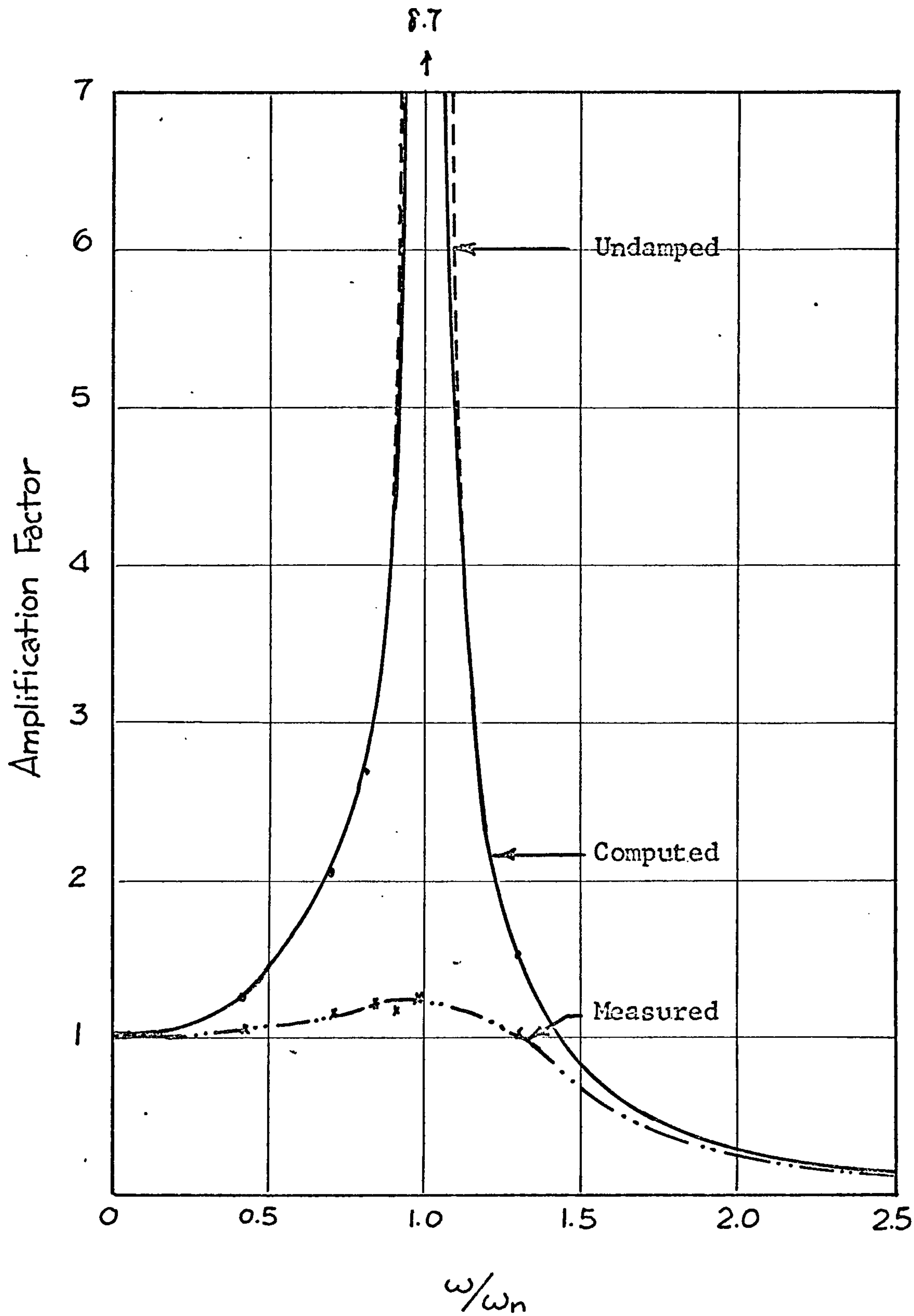

Fig. 29 Response of Copper-Manganese Shaft in Air Bearing

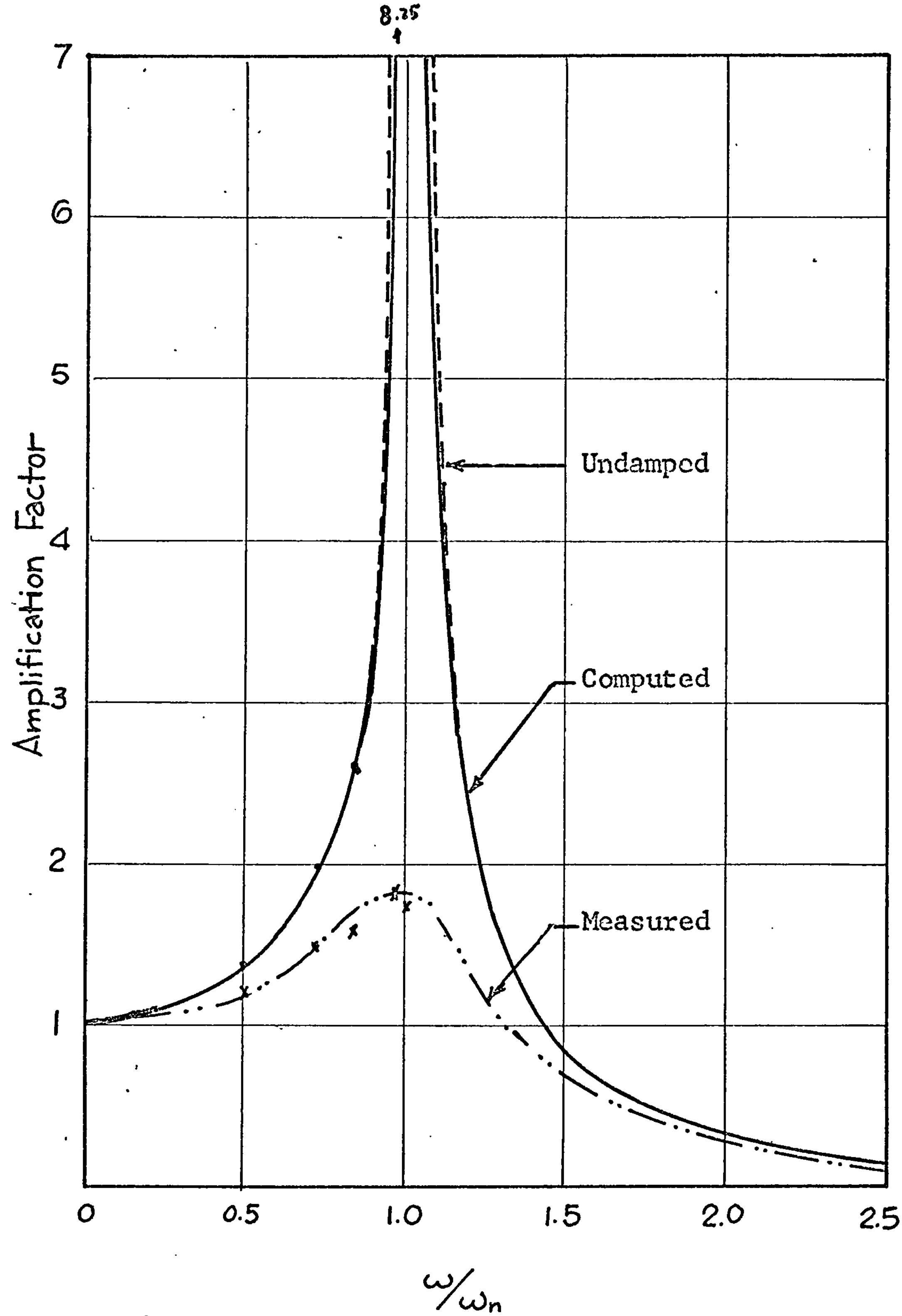

Fig. 30 Response of Aluminum-Alloy Shaft in Air Bearings

CHAPTER IV

ANALYSIS OF DATA

A rotating shaft system runs smoothly in its bearings and supporting system, if it is well aligned and lubricated, are characterized by different stiffness and damping. In combination with the mass of the disk this causes the critical speed for each case to occur at a different speed (see Table 2).

The effect of shaft stiffness and bearing type upon the critical speeds is shown in Table 6. The air bearing is stiffer than the oil-film bearing; both of these journal bearings are of approximately the same projected area, but the clearances in the air bearing are significantly less. This causes (for both cases) an end condition which is noticeably stiffer than that for the self-aligning ball bearing which is close to a simple support. If the journal bearings were close to being rigid supports (a fixed-fixed end condition), then the steel, copper-manganese alloy, and aluminum-alloy shafts would have critical speeds almost double the measured values (that is, 4870, 3200,and 2880 rpm, respectively). This suggests strongly that the restraint offered by the journal bearings is closer to that of a simple support than a fixed-end condition.

In Tables 3, 4, 5, and the associated Figures 22-30 respectively, the dimensionless response of the shaft systems

Table 6

Measured Critical Speeds

Bearing Type / Shaft Material	Journal		Self-aligning Ball
	Air-film (rpm)	Oil-film (rpm)	(rpm)
Steel ($E=30\times10^6$ psi)	2580	2475	1700 (1740)*
Copper-Manganese Alloy ($E=13\times10^6$ psi)	2000	1720	1110 (1145)
Aluminum Alloy ($E=10.5\times10^6$ psi)	1945	1650	1000 (1030)

* Computed

are shown and can be compared. The amplification factor A_R $(=1+\delta/\delta_{st})$ is the ratio of actual dynamic deflection of the shaft under the load of the disk alone. As such it gives a measure of the response of the shaft as the system passes through the speed range near the critical speed.

The computed response A_R is found by using a modified form of Equation (13), that is,

$$A_R = \frac{1}{\sqrt{\left[1-\left(\frac{\omega}{\omega_n}\right)^2\right]^2+\left(\frac{\omega}{\omega_n}\right)^2\left(\frac{c}{\omega_n}\right)^2}} \qquad (21)$$

where ω is the speed of rotation,

ω_n is the undamped critical speed $(=\sqrt{k/m})$, and

c is the (equivalent) viscous damping coefficient.

For the case discussed here, the last term is determined after (12) as in Appendix II.

The apparent discrepancy between the computed and measured values is particularly noticeable in near the critical speed. This is explained by the fact that the actual damping is affected significantly by rubbing which occurs at and near the critical speed but not at other speeds of rotation. The influence of the additional damping introduced in this way is manifested as very low measured values of the amplification factor in this sensitive speed range. Elsewhere the agreement is more reasonable.

Conclusions

From the results of this study we have confirmed that external damping (as supplied at the bearings) plays a important role in limiting the deflection amplitude of the shaft at or near the critical speed. Internal damping (present as natural damping in the shaft) does not play a significant role, but can limit the maximam speed at which a system can be driven.

BIBLIOGRAPHY

1. Tondl, A. <u>Some Problems of Rotor Dynamics</u> Chapter 1, (Chapman and Hall, London) 1965.

2. Muster, D. <u>Shock and Vibration Hand book</u> Vol. 3 1961, 39 "Balancing of Rotating Machinery".

3. Thmson, W. T. <u>Vibration Theory and Applications</u> Chapter 3, (Prentice Hall, Inc, Englewood Cliffs, N. J.)1965.

4. ________ 1, (Prentice Hall, Inc, Englewood Cliffs, N. J.) 1965.

5. Anongnous, "American Standaad Acoustical Terminology (Including Mechanical vibration), S 1.1 -1960 Page 16. United States of America Standards Institu e.

6. Sternlicht, B., H. Porisky, and E. Arwas: "Dynamic Stability Aspects of Cylindrical Journal Bearings Using Compressible and Incompressible Fluids," ONR Contract No. Nonr---2844(00), Task No. NR 097-348, 1960.

7. Kimball, A.L. 1925 Gen. Elect. Rev. Vol. 28, P. 554, "Measurement of Internal Friction in a Revolving Deflected Shaft."

8. ________ 1924 Gen. Elect. Rev. Vol. 27, P. 244, "Internal Friction Theory of Shaft Whirling."

9. Newkirk, B.L. 1924 Gen. Elect. Rev. Vol. 27, P. 169, "Shaft Whipping."

10. Kimball, A. 1. and Lovell, D. E. 1926 trans. ASME Vol. 48, p. 479, "Internal Friction in Solid."

11. Lazan, B. J. 1950 Trans. ASM Vol. 42, P. 499, "A Study with New Equipment of the Effects of Fatique Stress on the Damping Capacity and Elastivity of Mild Steel."

12. The Concept of Damping of Structureborne Sound and Vibration for Noise Control. Report to U.S. Navy Bureau of Ships. Report No. USN-1 April, 1961

13. Parkinson, A. G. etc. J. Mech.Engng. Sci., Vol. 5 1963, March, PP. 133- 145, "Some Experiment of the Balancing of Small Flexible Rotors, Part II."

14. Church, A. H. and Plankett, R. 1961 Nov. Trans. ASME, J. Engng. Indust. Vol. 838, PP.383-389, "Balancing Flexible Rotors."

APPENDIX I

THE EQUIVALENT VISCOUS DAMPING COEFFICIENT

The equivalent viscous damping coefficient for a damping force proportional to the square of the amplitude of vibration may be derived as follows (3).

Let the damping force be expressed by the equation

$$F_{eq}=\pm a\zeta^{2} \tag{22}$$

where the negative sign must be used when ζ is positive, and vice versa. Assuming harmonic motion with time measured from the position of extreme negative displacement, then,

$$\zeta=R\cos\omega t \tag{23}$$

The energy dissipated per cycle is

$$\begin{aligned} U &= \int F_{d}\,d\zeta \\ &= 2\int_{-R}^{R} a\zeta^{2}\,d\zeta \\ &= \frac{4}{3}\,aR^{3} \end{aligned} \tag{24}$$

But the work done percycle at resonance is

$$U=\pi C_{eq}\,\omega R^{2}$$

Therefore,

$$C_{eq}=\frac{4}{3\pi}a\omega R \tag{25}$$

where C_{eq} is the equivalent viscous damping coefficient and a is internal damping coefficient.

APPENDIX II

EVALUATION OF VISCOUS DAMPING COEFFICIENT

The viscous damping coefficients used in the computation of the amplification factors for each case were obtained as follows: By definition

$$c_c = 2m\,\omega_n \tag{26}$$

and

$$\psi = C/c_c = c/2\omega_n \tag{27}$$

where c is the decay constant $(=C/m)$. The amplification factor A_R is defined as (12)

$$A_R = \omega_A/c = 1 + \frac{\delta}{\delta_{st}} \tag{28}$$

where ω_A is the frequency of maximum amplitude. Thus,

$$c = \frac{\omega_A}{1 + \delta/\delta_{st}} \tag{29}$$

Using (29) in (21), we can compute values of the amplification factor with which to compare the measured values.

For the three cases cited here the corresponding values of c are

Self-aligning Bearing .... c=35.1 (in^2/sec^3)

Oil-film Journal Bearing .... c=26.0

Air-Bearing .... c=24.0